Iterative Learning Hybrid Robust Predictive Control for Multi-Phase Batch Processes with Asynchronous Switching via a Lyapunov-Razumikhin Approach

Hui Li, Shiqi Wang, Huiyuan Shi, Ping Li, *Senior Member, IEEE*, and Chengli Su, *Member, IEEE*

***Abstract*—For a class of the industrial cyber-physical system, i.e., multi-phase batch processes with small time-delays and asynchronous switching, this study develops a two-dimensional iterative learning hybrid robust predictive control method. Compared with the previous Lyapunov-Krasovsky function-based method, stability conditions given by the Lyapunov-Razumikhin function-based method is less conservative intensive in dealing with small time-delays. Not only that, compared to the traditional iterative learning method, the rolling-optimized gains of the control law make it possible for the designed controller to have fewer learning cycles, and the control performance is even better. Meanwhile, the minimum and the maximum dwelling times are obtained in conjunction with the exponential stability analysis of the system. Since the obtained dwelling times, an advanced switching signal is provided to avoid asynchronous switching situations. The simulation results for the injection molding process are finally utilized to illustrate the effectiveness and feasibility of the developed approach.**

***Index Terms*—Asynchronous switching, iterative learning control, model predictive control, multi-phase batch process, small time-delay, industrial cyber-physical system.**

Manuscript received 21 March 2023; revised 8 June 2023 and 16 August 2023; accepted 7 October 2023. Date of publication 13 October 2023; date of current version 17 November 2023. This work was supported in part by the National Natural Science Foundation of China under Grant 62203202, in part by the Natural Science Foundation of Liaoning Province under Grant 2022-BS-295, in part by the Youth Project of the Educational Department of Liaoning Province under Grant LJKQZ20222432, and in part by the Graduate Science and Technology Innovation Program of the University of Science and Technology Liaoning under Grant LKDYC202201. *(Corresponding authors: Huiyuan Shi; Ping Li.)*

Hui Li, Shiqi Wang, and Ping Li are with the School of Electronics and Information Engineering, University of Science and Technology Liaoning, Anshan 114051, China (e-mail: lihui2113@foxmail.com; wangshiqi918@gmail.com; liping@lnpu.edu.cn).

Huiyuan Shi is with the School of Information and Control Engineering, Liaoning Petrochemical University, Fushun 113001, China, and also with the State Key Laboratory of Synthetical Automation for Process Industries, Northeastern University, Shenyang 110819, China (e-mail: shy723915@126.com).

Chengli Su is with the School of Information and Control Engineering, Liaoning Petrochemical University, Fushun 113001, China, and also with the School of Information Engineering, Liaodong University, Dandong 118001, China (e-mail: sclwind@sina.com).

Digital Object Identifier 10.1109/TICPS.2023.3324616

I. Introduction

DUE to its high value-added and small-scale features, batch processes have quickly risen in prominence as one of the primary manufacturing processes. Rapidly, pertinent theories and control technologies were developed [1], [2], [3], [4], [5], [6]. However, both the early iterative learning control (ILC) methods [7], [8], [9] and the one-dimensional model predictive control methods [10], [11], [12] have inherent limitations that make it difficult to improve control performance. For batch processes with two-dimensional (2D) characteristics, existing ILC methods have difficulty coping with the non-repetitive disturbances and require a lengthy learning cycle, while the one-dimensional model predictive control methods lack batch direction optimization and have poor control accuracy. Consequently, the iterative learning model predictive control [13], [14], [15] methods, combining the advantages of both ILC and model predictive control methods, have been investigated, which fully take into account the 2D characteristics and can effectively cope with the effects of uncertainties and disturbances. In references [13], [14], [15], the real-time feedback had been incorporated into the ILC design, which reduces to some extent the problem of lengthy learning cycles and improves the tracking performance from the initial cycles. Regrettably, these methods are an offline solution method, i.e., the control law gain is fixed for each batch. The fixed control law gain cannot effectively respond to the real-time dynamic characteristics of the system. As a result, the learning cycle cannot be significantly shortened even if the real-time feedback information of the system is considered.

Notably, in actual production, multi-phase batch processes (MPBP) are much more common. Due to the late start of related studies for MPBP, the research results are not significant. In 2008, a 2D iterative learning model predictive control strategy was discussed in [16] for MPBP. The study of [17] develops an iterative learning model predictive control approach with a 2D convergence index. In addition, other investigations on MPBP are either found in [18], [19], [20] as well. Nevertheless, the investigations in [16], [17], [18], [19], [20] for MPBP focus on the synchronous switching way, that is, system states and controllers are switched simultaneously. In fact, this is unlikely. Owing to the system's recognition speed, the latency in signal

transmission, and other variables, the system states and controllers stay synchronous when switching occurs. This issue is further exemplified in some studies with asynchronous switching. A class of robust model predictive schemes that depend on the model-dependent average dwell time technique are discussed in [21]. Similar studies can be found in [22] and [23]. Unfortunately, the methods [21], [22], [23] do not sufficiently consider the system's 2D characteristics. Because the optimization in the batch direction is missing, the control accuracy doesn't get better as the operating cycles increase. Hence, Wang et al. [24] put forward a 2D-ILC method for MPBP, which effectively utilizes batch information and improves control accuracy. However, the gains of the control law and switching parameters obtained in an offline way are fixed. Because of this, the controller requires enough operating cycles to stably track the setpoint. Not only that, with the operation of the system, the fixed switching parameters will make the error between the actual switching time and the solved switching time larger, leading to a bigger fluctuation of the system during switching. Therefore, it is worthwhile to study deeply how to reduce the learning cycles and suppress the large fluctuations during switching.

Additionally, time-delays are also one of the issues that need to be considered in MPBP. In previous investigations [21], [25], [26], [27], [28], the treatment of time-delays usually utilizes the upper and lower bound information of time-delays to redesign the Lyapunov-Krasovsky function (LKF). The controller designed in this way will inevitably be more conservative. Nevertheless, the conservatism brought by the LKF method is acceptable in large time-delayed systems. After all, it can significantly reduce the computational effort. In small time-delayed systems, the disadvantage of LKF becomes obvious, where it is neither possible to circumvent the problem of large conservatism nor to effectively reduce the computational effort. Consequently, the approaches to the Lyapunov-Razumikhin function (LRF) [28], [29], [30] were noted. In the LRF method, the dimensionality of V-function is directly related to the size of the time-delays. The smaller time-delays, the smaller dimensionality of the designed function, and the lower the conservativeness. Therefore, the LRF method based on the dimensional expansion way is more advantageous compared to the LKF method. Regretfully, few studies based on LRF have been reported for MPBP with small time-delays.

Synthesizing the preceding exposition, a 2D iterative learning hybrid robust predictive control (ILHRPC) method is developed for MPBP with small time-delays and asynchronous switching. First, a multi-delay model is utilized to describe MPBP. On the basis of the model above, by using the state deviation and output error, a novel 2D Roesser comprehensive feedback error switching model is constructed. Then, based on the switching model, an ILHRPC law is designed. Second, by solving the stability conditions in the form of the linear matrix inequality (LMI), which are given by the terminal constraints set and the exponential stability analysis, the real-time gains of the control law, minimum dwelling time (Min-DT) for the match case, and maximum dwelling time (Max-DT) for the mismatch case, are solved. Based on the dwelling times, the advanced signal is given to avoid the asynchronous switching situations when switching occurs. In the end, the developed approach is effective and feasible through a simulation study.

The main advantages of this method include: 1) When switching occurs, the system's fluctuations are effectively suppressed via online optimization of the switching coefficients to dynamic adjustment of the switching time. 2) The gains of the control law solved online by rolling optimization resultful reduce the learning cycles of the controller and enhance the control performance. 3) For MPBP with small time-delays, stability conditions based on the LRF method are less conservative and less computationally intensive to solve than the LKF method.

Notations: $\mathcal{F}$ and κ denote time index and batch indexes. $x(\mathcal{F},\kappa)\in\mathbb{R}^{n_x^p}, y(\mathcal{F},\kappa)\in\mathbb{R}^{n_y^p}, u(\mathcal{F},\kappa)\in\mathbb{R}^{n_u^p}$ and $\omega(\mathcal{F},\kappa)\in\mathbb{R}^{n_\omega^p}$ denote the state, output, input, and disturbances, respectively. n_x^p, n_y^p, n_u^p and n_ω^p are the suitable dimension at the p-th phase. $\ell:\mathbb{Z}_+\times\mathbb{Z}_+\to\{1,2,\ldots,p,\ldots,P\}$ stands a switching signal. I^p is a constant matrix with appropriate dimension. $\mathfrak{M}_S^p$ denotes the Min-RT and $\mathfrak{M}_U^p$ denotes the Max-RT. d_M stands time delays.

II. Problem Formulation

The MPBP below with uncertainties, disturbances, and time delays is:

$$\begin{cases} x(\mathcal{F}+1,\kappa)=\sum_{\mathcal{G}=-d_M}^{0}A_{\mathcal{G}}^{\ell}(\mathcal{F},\kappa)x(\mathcal{F}+\mathcal{G},\kappa)\\ +B^{\ell}(\mathcal{F},\kappa)u(\mathcal{F},\kappa)\\ +\omega^{\ell}(\mathcal{F},\kappa)\\ y(\mathcal{F},\kappa)=C^{\ell}x(\mathcal{F},\kappa)\end{cases}\tag{1}$$

Considering situations where system states mismatch controllers when switching occurs, a system switching model with the match and mismatch cases can be represented as

$$\begin{cases} x^p(\mathcal{F}+1,\kappa)=\sum_{\mathcal{G}=-d_M}^{0}A_g^p(\mathcal{F},\kappa)x^p(\mathcal{F}+\mathcal{G},\kappa)\\ +B^p(\mathcal{F},\kappa)u^p(\mathcal{F},\kappa)+\omega^p(\mathcal{F},\kappa)\\ y^p(\mathcal{F},\kappa=C^px^p(\mathcal{F},\kappa)\end{cases}\quad(a)$$

$$\begin{cases} x^p(\mathcal{F}+1,\kappa)=\sum_{\mathcal{G}=-d_M}^{0}A_g^p(\mathcal{F},\kappa)x^p(\mathcal{F}+\mathcal{G},\kappa)\\ +B^p(\mathcal{F},\kappa)u^{p-1}(\mathcal{F},\kappa)+\omega^p(\mathcal{F},\kappa)\\ y^p(\mathcal{F},\kappa)=C^px^p(\mathcal{F},\kappa)\end{cases}\quad(b)\tag{2}$$

where $A_g^p(\mathcal{F},\kappa)$ and $B^p(\mathcal{F},\kappa)$ denote respectively state and input uncertainty matrixes, which satisfying $A_g^p(\mathcal{F},\kappa)=A_g^p+\Delta_a^p(\mathcal{F},\kappa), B^p(\mathcal{F},\kappa)=B^p+\Delta_b^p(\mathcal{F},\kappa), \Delta_a^p(\mathcal{F},\kappa)=N^p\Delta^p(\mathcal{F},\kappa)H_b^p$ and $\Delta_b^p(\mathcal{F},\kappa)=N^p\Delta^p(\mathcal{F},\kappa)H_b^p$. $\{A_g^p,B^p\}$ are the state and input constant matrices. $\{N^p,H_a^p,H_b^p\}$ are the real constant matrixes with appropriate dimensions. $\Delta(t,k)$ denotes the uncertainty matrix, which satisfies $\Delta^p(\mathcal{F},\kappa)^{\mathrm{T}}\Delta^p(\mathcal{F},\kappa)\le I^p$. $\omega(\mathcal{F},\kappa)$ denotes unknow external disturbance.

Furthermore, the switching condition of the system states of adjacent phases can be described as

$$\ell=\begin{cases}\ell+1 & \text{if } \partial^{p+1}(x(\mathcal{F},\kappa))<0\\ \ell & \text{others}\end{cases}\tag{3}$$

where $\partial^{p+1}(x(\mathcal{F},\kappa))$ is a switching case. Meanwhile, the switching time $\bar{T}^p$ satisfy:

$$\bar{\mathcal{F}}^p=\min\left\{t>\bar{\mathcal{F}}^{p-1}|\partial^p(x(\mathfrak{F},\mathfrak{K}))<0\right\},\bar{\mathcal{F}}^0=0\tag{4}$$

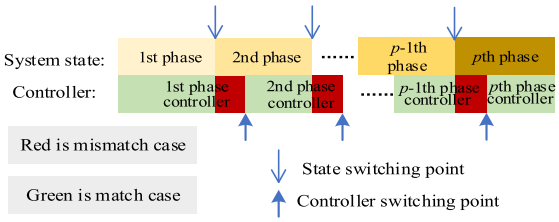

Fig. 1. Operating process of the system with asynchronous switching situations.

Moreover, $(\bar{\mathcal{F}}^p, \kappa_k)$ and $\ell(\bar{\mathcal{F}}^p, \kappa_k)$ are the time interval and the switching point. Then, for the overall operation time, the switching sequence are:

$$\begin{aligned}\sum = \big\langle &(\bar{\mathcal{F}}^{1S}, \kappa_1), \ell(\bar{\mathcal{F}}^{1S}, \kappa_1), (\bar{\mathcal{F}}^{2U}, \kappa_1)\ , \\ &\ell(\bar{\mathcal{F}}^{2U}, \kappa_1)(\bar{\mathcal{F}}^{2S}, \kappa_1), \ell(\bar{\mathcal{F}}^{2S}, \kappa_1), \\ &\ldots, (\bar{\mathcal{F}}^{pS}, \kappa_1), \ell(\bar{\mathcal{F}}^{pS}, \kappa_1), (\bar{\mathcal{F}}^{1S}, \kappa_2), \\ &\ell(\bar{\mathcal{F}}^{1S}, \kappa_2), \ldots, (\bar{\mathcal{F}}^{pS}, \kappa_2), \\ &\ell(\bar{\mathcal{F}}^{pS}, \kappa_2) \ldots (\bar{\mathcal{F}}^{1S}, \kappa_k), \ell(\bar{\mathcal{F}}^{1S}, \kappa_k), \ldots, \\ &(\bar{\mathcal{F}}^{pS}, \kappa_k), \ell(\bar{\mathcal{F}}^{pS}, \kappa_k)\big\rangle \end{aligned} \tag{5}$$

where $(\bar{\mathcal{F}}^{pS}, \kappa_k)$ and $(\bar{\mathcal{F}}^{pU}, \kappa_k)$ stand dwelling times at discrete $\mathcal{F}$ time in the κ batch under the match and the mismatch cases, respectively. $\ell(\bar{\mathcal{F}}^{pS}, \kappa_k)$ and $\ell(\bar{\mathcal{F}}^{pU}, \kappa_k)$ are state and controller switching points. The switching signal satisfies $\bar{\mathcal{F}}^{pS} - \bar{\mathcal{F}}^{pU} \geq \mathfrak{M}_S^p$, $\bar{\mathcal{F}}^{pU} - \bar{\mathcal{F}}^{(p-1)U} \leq \mathfrak{M}_U^p$. Moreover, the relationship of the adjacent phase can be described as

$$x^p(\mathcal{F}^{p-1}, \kappa) = \boldsymbol{a}^p x^{p-1}(\mathcal{F}^{p-1}, \kappa) \tag{6}$$

where $\boldsymbol{a}^p$ is state-transition matrix. $\boldsymbol{a}^p$ is usually obtained from the relationship between the two phases in practice. If the dimension of adjacent phase states is the same, then $\boldsymbol{a}^p$ is equivalent to I^P.

Remark 1: Within the batch processes, a batch is usually divided into multiple phases because of the different production purposes and the different mechanisms of system operation. In addition, the system is influenced by some factors when switching between phases, and asynchronous switching situations may occur. The asynchronous switching situation can be considered a delay in information between the computing component and the physical hardware used for control. When a certain condition is satisfied, the system will transition to the next phase and the computing component gives a switching signal immediately. Since the inherent complexity and external disturbance of MPBP, the switching signal cannot be transmitted to the physical hardware for control without delay. For that reason, if the system state meets switching conditions, it is vital to precisely predict the time required (Min-DT) and the signal delay time (Max-DT), which can effectively avoid asynchronous switching situations. From Fig. 1, the operating process of the system with asynchronous switching situations is given.

III. Controller Design

A. 2D Roesser Comprehensive Feedback Error Model

In this part, a 2D Roesser comprehensive feedback error model is designed, which includes state deviation along the batch direction and output error along the time direction. It can provide sufficient information for the designed controller.

First, we need to define the output error as follows.

$$e^p(\mathcal{F}, \kappa) = y^p(\mathcal{F}, \kappa) - y_r^p \tag{7}$$

where y_r^p represents set values.

Then, the following control law is defined:

$$\begin{cases} u(\mathcal{F}, \kappa) = u(\mathcal{F}, \kappa - 1) + r(\mathcal{F}, \kappa) \\ u(\mathcal{F}, 0) = 0 \end{cases} \tag{8}$$

Second, we define the incremental function along the batch direction as $\Delta f(\mathcal{F}, \kappa) = f(\mathcal{F}, \kappa) - f(\mathcal{F}, \kappa - 1)$, where f may denote states, output, or disturbance. Hence, the state deviation and output error are:

$$\begin{cases} \Delta x^p(\mathcal{F}+1, \kappa) = \sum_{\mathcal{G}=-d_M}^{0} A_{\mathcal{G}}(\mathcal{F}, \kappa)\Delta x^p(\mathcal{F}, \kappa) \\ +B^{pi}(\mathcal{F}, \kappa)r^p(\mathcal{F}, \kappa)) + \bar{\omega}^p(\mathcal{F}, \kappa); \\ \Delta x^p(\mathcal{F}+1, \kappa) = \sum_{\mathcal{G}=-d_M}^{0} A_{\mathcal{G}}(\mathcal{F}, \kappa)\Delta x^p(\mathcal{F}, \kappa) \\ +B^{pi}(\mathcal{F}, \kappa)r^{p-1}(\mathcal{F}, \kappa)) + \bar{\omega}^p(\mathcal{F}, \kappa) \end{cases}$$

$$\begin{cases} e^p(\mathcal{F}+1, \kappa) = e^p(\mathcal{F}+1, \kappa-1) + C\Delta x(\mathcal{F}+1, \kappa) \\ = e^p(\mathcal{F}+1, \kappa-1) + C(\sum_{\mathcal{G}=-d_M}^{0} A_{\mathcal{G}}(\mathcal{F}, \kappa)\Delta x^p(\mathcal{F}, \kappa) \\ +B^{pi}(\mathcal{F}, \kappa)r^p(\mathcal{F}, \kappa)) + \bar{\omega}^{pS}(\mathcal{F}, \kappa)) \\ e^p(\mathcal{F}+1, \kappa) = e^p(\mathcal{F}+1, \kappa-1) + C\Delta x(\mathcal{F}+1, \kappa) \\ = e^p(\mathcal{F}+1, \kappa-1) + C(\sum_{\mathcal{G}=-d_M}^{0} A_g(\mathcal{F}, \kappa)\Delta x^p(\mathcal{F}, \kappa) \\ +B^{pi}(\mathcal{F}, \kappa)r^{p-1}(\mathcal{F}, \kappa)) + \bar{\omega}^{pU}(\mathcal{F}, \kappa)) \end{cases} \tag{9}$$

where $\bar{\omega}^{pS}(\mathcal{F}, \kappa) = (\Delta_a^p(\mathcal{F}, \kappa) - \Delta_a^p(\mathcal{F}, \kappa - 1))x^p(\mathcal{F}, \kappa - 1) + (\Delta_b^p(\mathcal{F}, \kappa) - \Delta_b^p(\mathcal{F}, \kappa - 1))u^p(\mathcal{F}, \kappa - 1) + \Delta\omega^p(\mathcal{F}, \kappa)$, $\bar{\omega}^{pU}(\mathcal{F}, \kappa) = (\Delta_a^p(\mathcal{F}, \kappa) - \Delta_a^p(\mathcal{F}, \kappa - 1))x^p(\mathcal{F}, \kappa - 1) + (\Delta_b^p(\mathcal{F}, \kappa) - \Delta_b^p(\mathcal{F}, \kappa - 1))u^{p-1}(\mathcal{F}, \kappa - 1) + \Delta\omega^p(\mathcal{F}, \kappa)$. Since $\bar{\omega}^{pS}(\mathcal{F}, \kappa)$ and $\bar{\omega}^{pU}(\mathcal{F}, \kappa)$ are unknown bounded disturbances, we consider their ranges to be the same, i.e., $\bar{\omega}^{pS}(\mathcal{F}, \kappa) = \bar{\omega}^{pU}(\mathcal{F}, \kappa) = \bar{\omega}^p(\mathcal{F}, \kappa)$.

On the basis of (9), a 2D Roesser comprehensive feedback error model is:

$$\begin{cases} \bar{x}^p(\mathcal{F}+1, \kappa) = \bar{A}_0^p(\mathcal{F}, \kappa)\bar{x}^p(\mathcal{F}, \kappa) + \sum_{\mathcal{G}=-d_M, \bar{b}=-b_M}^{-1} \\ \bar{A}_{\mathcal{G}}^p(\mathcal{F}, \kappa)\bar{x}^p(\mathcal{F}+\mathcal{G}, \kappa+\bar{b}) \\ + \bar{B}^p(\mathcal{F}, \kappa)r^p(\mathcal{F}, \kappa) + D\bar{\omega}^p(\mathcal{F}, \kappa) \\ \Delta y^p(\mathcal{F}, \kappa) = \bar{C}^p\bar{x}^p(\mathcal{F}, \kappa) \end{cases} \tag{a}$$

$$\begin{cases} \bar{x}^p(\mathcal{F}+1, \kappa) = \bar{A}_0^p(\mathcal{F}, \kappa)\bar{x}^p(\mathcal{F}, \kappa) + \sum_{\mathcal{G}=-d_M, \bar{b}=-b_M}^{0} \\ \bar{A}_{\mathcal{G}}^p(\mathcal{F}, \kappa)\bar{x}^p(\mathcal{F}+\mathcal{G}, \kappa+\bar{b}) \\ + \bar{B}^p(\mathcal{F}, \kappa)r^{p-1}(\mathcal{F}, \kappa) + D\bar{\omega}^p(\mathcal{F}, \kappa) \\ \Delta y^p(\mathcal{F}, \kappa) = \bar{C}^p\bar{x}^p(\mathcal{F}, \kappa) \end{cases} \tag{b}$$

(10)

where $\bar{A}_0^p(\mathcal{F}, \kappa) = \bar{A}_0^p + \bar{N}^p\Delta^p(\mathcal{F}, \kappa)\bar{H}_a^p$, $\bar{A}_g^p(\mathcal{F}, \kappa) = \bar{A}_g^p + \bar{N}^p\Delta^p(\mathcal{F}, \kappa)\bar{H}_a^p$, $\bar{B}^p(\mathcal{F}, \kappa) = \bar{B}^p + \bar{N}^p\Delta^p(\mathcal{F}, \kappa)\bar{H}_b^p$, $\bar{A}_{0,q} = \begin{bmatrix} A^p & 0 \\ CA^p & I \end{bmatrix}$, $\bar{A}_{\mathcal{G}}^p = \begin{bmatrix} A_{\mathcal{G}}^p & 0 \\ C^pA_{\mathcal{G}}^p & 0 \end{bmatrix}$, $\bar{B}^p = \begin{bmatrix} B^p \\ C^p\bar{B}^p \end{bmatrix}$, $D =$

$\begin{bmatrix} I^p \\ C^p \end{bmatrix}, \bar{N}^p = \begin{bmatrix} N^p \\ C^p N^p \end{bmatrix}, \bar{H}_a^p = \begin{bmatrix} H_a^p & 0 \\ H_b^p & 0 \end{bmatrix}, \bar{x}^p(\mathcal{F}+1,\kappa) = \begin{bmatrix} \Delta x^p(\mathcal{F}+1,\kappa) \\ e^p(\mathcal{F}+1,\kappa) \end{bmatrix} = \begin{bmatrix} \bar{x}^h(\mathcal{F}+1,\kappa) \\ \bar{x}^v(\mathcal{F},\kappa+1) \end{bmatrix}, \bar{x}^p(\mathcal{F},\kappa) = \begin{bmatrix} \Delta x^p(\mathcal{F},\kappa) \\ e^p(\mathcal{F}+1,\kappa-1) \end{bmatrix} = \begin{bmatrix} \bar{x}^h(\mathcal{F},\kappa) \\ \bar{x}^v(\mathcal{F},\kappa) \end{bmatrix}, \quad \bar{x}^p(\mathcal{F}+\mathcal{G},\kappa+\bar{b}) = \begin{bmatrix} \bar{x}^h(\mathcal{F}+\mathcal{G},\kappa) \\ \bar{x}^v(\mathcal{F},\kappa+\bar{b}) \end{bmatrix} = \begin{bmatrix} \Delta x^p(\mathcal{F}+\mathcal{G},\kappa) \\ e^p(\mathcal{F}+1,\kappa-1+\bar{b}) \end{bmatrix}, \mathcal{G} \in \mathbb{Z}_{[-d_M,0]}, \bar{b} \in \mathbb{Z}_{[-b_M,0]}.$

B. Design of ILHRPC Law

From (6), the relationship between the state of the adjacent phase below can be described.

$$\begin{aligned} &\begin{bmatrix} \Delta x^{p+1}(\bar{\mathcal{F}}_k^p,\kappa) \\ e^{p+1}(\bar{\mathcal{F}}_k^p,\kappa) \end{bmatrix} \\ &= \begin{bmatrix} \boldsymbol{a}^p \Delta x^p(\bar{\mathcal{F}}_k^p,\kappa) \\ C^p \boldsymbol{a}^p(\Delta x^p(\bar{\mathcal{F}}_k^p,\kappa) + x^p(\bar{\mathcal{F}}_k^p-1,\kappa)) - y_r^p \end{bmatrix} \\ &= \begin{bmatrix} \boldsymbol{a}^p \\ C^p \boldsymbol{a}^p \end{bmatrix} \begin{bmatrix} I & 0 \end{bmatrix} \begin{bmatrix} \Delta x^p(\bar{\mathcal{F}}_k^p,\kappa) \\ e^p(\bar{\mathcal{F}}_k^p,\kappa) \end{bmatrix} \\ &\quad + \begin{bmatrix} 0 \\ C^p \boldsymbol{a}^p x^p(\bar{\mathcal{F}}_k^p,\kappa-1) - y_r^p \end{bmatrix} \end{aligned} \tag{11}$$

Then, $\bar{x}^{p+1}(\bar{\mathcal{F}}_k^p,\kappa) = \bar{\boldsymbol{a}}^p \bar{x}^p(\bar{\mathcal{F}}_k^p,\kappa) + \spadesuit^p$ can be obtained, where $\bar{\boldsymbol{a}}^p = \begin{bmatrix} \boldsymbol{a}^p \\ C^p \boldsymbol{a}^p \end{bmatrix}$, $\spadesuit^p = \begin{bmatrix} 0 \\ C^p \boldsymbol{a}^p x^p(\bar{\mathcal{F}}_k^p,\kappa-1) - y_r^\rho \end{bmatrix}$, and $\bar{\mathcal{F}}_k^p = \bar{\mathcal{F}}_{k-1}^p$. Based on (8b), considering the time and batch directions information, the ILHRPC law is designed.

$$\begin{aligned} &r^p(\mathcal{F}+\zeta|\mathcal{F},\kappa+k|\kappa) \\ &= F^p \begin{bmatrix} \Delta x^p(\mathcal{F}+\zeta|\mathcal{F},\kappa+k|\kappa) \\ e^p(\mathcal{F}+1+\zeta|\mathcal{F},\kappa-1+k|\kappa) \end{bmatrix} \\ &= F^p \bar{x}^p(\mathcal{F}+\zeta|\mathcal{F},\kappa+k|\kappa); \\ &r^{p-1}(\mathcal{F}+\zeta|\mathcal{F},\kappa+k|\kappa) \\ &= F^{p-1} \begin{bmatrix} \Delta x^{p-1}(\mathcal{F}+\zeta|\mathcal{F},\kappa+k|\kappa) \\ e^{p-1}(\mathcal{F}+1+\zeta|\mathcal{F},\kappa-1+k|\kappa) \end{bmatrix} \\ &= F^{p-1} \bar{x}^{p-1}(\mathcal{F}+\zeta|\mathcal{F},\kappa+k|\kappa) \\ &= F^{p-1}(\bar{\boldsymbol{a}}^{p-1})^{-1} \bar{x}^p(\kappa+\zeta|\kappa,\kappa+k|\kappa) \end{aligned} \tag{12}$$

where F^p and F^{p-1} are the control law gains at the p-th phase and (p-1)-th phase, respectively. ζ and k represent prediction steps in time and batch directions, respectively.

Based on (10) and (12), a closed loop 2D Roesser comprehensive feedback error model can be obtained below.

$$\begin{cases} \bar{x}^p(\mathcal{F}+1,\kappa) = \bar{A}_{\mathcal{G}}^p(\mathcal{F},\kappa)\bar{x}^p(\mathcal{F},\kappa) + \sum_{\mathcal{G}=-d_M,\bar{b}=-b_M}^{0} \\ \bar{A}_{\mathcal{G}}^p(\mathcal{F},\kappa)\bar{x}^p(\mathcal{F}+\mathcal{G},\kappa+\bar{b}) \\ \quad + \bar{B}^p(\mathcal{F},\kappa)F^p\bar{x}^p(\mathcal{F},\kappa) + D\bar{\omega}^p(\mathcal{F},\kappa) \\ \Delta y^p(\mathcal{F},\kappa) = \bar{C}^p\bar{x}^p(\mathcal{F},\kappa) \\ z^p(\mathcal{F},\kappa) \triangleq e^p(\mathcal{F},\kappa) = E^p\bar{x}^p(\mathcal{F},\kappa) \end{cases} \tag{a}$$

$$\begin{cases} \bar{x}^p(\mathcal{F}+1,\kappa) = \bar{A}_{\mathcal{G}}^p(\mathcal{F},\kappa)\bar{x}^p(\mathcal{F},\kappa) + \sum_{\mathcal{G}=-d_M,\bar{b}=-b_M}^{0} \\ \bar{A}_{\mathcal{G}}^p(\mathcal{F},\kappa)\bar{x}^p(\mathcal{F}+\mathcal{G},\kappa+\bar{b}) \\ \quad + \bar{B}^p(\mathcal{F},\kappa)F^{p-1}(\bar{\boldsymbol{a}}^{p-1})^{-1}\bar{x}^p(\mathcal{F},\kappa) + D\bar{\omega}^p(\mathcal{F},\kappa) \\ \Delta y^p(\mathcal{F},\kappa) = \bar{C}^p\bar{x}^p(\mathcal{F},\kappa) \\ z^p(\mathcal{F},\kappa) \triangleq e^p(\mathcal{F},\kappa) = E^p\bar{x}^p(\mathcal{F},\kappa) \end{cases} \tag{b}$$

(13)

Afterward, the following robust model predictive control (RMPC) finite optimal cost function is given and the RMPC optimization problem is described.

$$\begin{aligned} &\min_{r^p(\mathcal{F}+\zeta|\mathcal{F},\kappa+k|\kappa),\mathcal{G},\bar{b}\geq 0} \ \max_{[\bar{A}_{\mathcal{G}}^p(\mathcal{F},\kappa)\bar{B}^p(\mathcal{F},\kappa)\bar{\omega}(\mathcal{F},\kappa)]} J_\infty^p(\mathcal{F},\kappa) \\ &J_\infty^p(\mathcal{F},\kappa) = \sum_{l=0}^{N-1}\sum_{m=0}^{N-1} \\ &\times \big[\bar{x}^{p\mathrm{T}}(\mathcal{F}+\zeta|\mathcal{F},\kappa+k|\kappa)Q^p\bar{x}^p(\mathcal{F}+\zeta|\mathcal{F},\kappa+k|\kappa) \\ &\quad + r^{p\mathrm{T}}(\mathcal{F}+\zeta|\mathcal{F},\kappa+k|\kappa)R^p r^p(\mathcal{F}+\zeta|\mathcal{F},\kappa+k|\kappa) \\ &\quad - \tau\bar{\omega}^{p\mathrm{T}}(\mathcal{F}+\zeta|\mathcal{F},\kappa+k|\kappa) \\ &\quad \bar{\omega}^p(\mathcal{F}+\zeta|\mathcal{F},\kappa+k|\kappa)\big] + V_T(\bar{x}^p(\mathcal{F}+N|\mathcal{F},\kappa+N|\kappa)) \end{aligned} \tag{14}$$

$$\begin{aligned} &s.t. \\ &\bar{x}^p(\mathcal{F}+\zeta,\kappa+k) \in \Omega_t, r \in \bar{R} := \{r||r_k| \leq r_{k,\max}\}, \bar{\omega} \in W \\ &:= \{\bar{\omega}|\bar{\omega}^{\mathrm{T}}\bar{\omega} \leq \eta^2\}. \end{aligned}$$

Where Q^p and R^p denote the state weighting matrix and tracking weighting matrix, respectively. τ is a positive scalar and $V_T(\bar{x}^p(\mathcal{F}+N|\mathcal{F},\kappa+N|\kappa))$ is a terminal cost. η denotes a known constant and r_k is the k element of the predictive control law.

Remark 2: In the previous iterative learning model predictive control method for MPBP, to reduce the computational cost, the gains of the control law is calculated offline. Therefore, the optimization problem becomes less feasible. To this end, these studies optimize the controller by using historical control input information to partially enhance the control performance of the system. However, this means that the controller necessarily requires a lengthy learning cycle. Hence, based on the (8) and (12), we have $u^p(\mathcal{F},\kappa) = u^p(\mathcal{F},\kappa-1) + F^p\bar{x}^p(\mathcal{F},\kappa)$, $u^{p-1}(\mathcal{F},\kappa) = u^{p-1}(\mathcal{F},\kappa-1) + F^{p-1}(\bar{\boldsymbol{a}}^{p-1})^{-1}\bar{x}^p(\mathcal{F},\kappa)$.

We use an online solution for rolling optimization of the decision variables F^p and F^{p-1}, while combining historical control input information $u(t,k-1)$ to resultful enhance the control performance and reduce learning cycles of the controller.

C. Main Results

The stability conditions are provided, which is relying on the robust positively invariant (RPI) set and terminal constraint set. By solving these conditions, we can obtain the gains of the ILHRPC law.

RPI:

Definition 1: Typically, we denote $\Omega \subseteq \mathrm{X}$ as a RPI set and $r^p(\mathcal{F},\kappa)$ as the iterative predictive control law. The RPI set is expressed as $\bar{x}^p(\mathcal{F}+\mathcal{G},\kappa+\bar{b}) \in \Omega$. For the 2D switching system (13), Ω is

$$\Omega = \left\{x | V(\bar{x}^p(\mathcal{F}+\mathcal{G},\kappa+\bar{b})) \le \xi\right\} \tag{15}$$

The iterative predictive control law is:

$$r^p(\mathcal{F},\kappa) = F^p \bar{x}^p(\mathcal{F},\kappa) \tag{16}$$

Moreover, the LRF is defined as

$$\begin{aligned}
&V_S(\bar{x}^p(\mathcal{F},\kappa))\\
&\quad = \bar{x}^{p\mathrm{T}}(\mathcal{F},\kappa)P^p\bar{x}^p(\mathcal{F},\kappa) = \bar{x}^{p\mathrm{T}}(\mathcal{F},\kappa)P^{ph}\bar{x}^p(\mathcal{F},\kappa)\\
&\quad + \bar{x}^{p\mathrm{T}}(\mathcal{F},\kappa)P^{pv}\bar{x}^p(\mathcal{F},\kappa),\\
&V_U(\bar{x}^p(\mathcal{F},\kappa)) = \bar{x}^{p\mathrm{T}}(\mathcal{F},\kappa)P^{p-1}\bar{x}^p(\mathcal{F},\kappa)\\
&\quad = \bar{x}^{p\mathrm{T}}(\mathcal{F},\kappa)P^{(p-1)h}\bar{x}^p(\mathcal{F},\kappa)\\
&\quad + \bar{x}^{p\mathrm{T}}(\mathcal{F},\kappa)P^{(p-1)v}\bar{x}^p(\mathcal{F},\kappa),\\
&P^p = \mathrm{diag}[P^{ph}, P^{pv}], P^{p-1} = \mathrm{diag}[P^{(p-1)h}, P^{(p-1)v}],
\end{aligned}$$

where S and U is the match and mismatch cases, respectively.

Lemma 1: The Ω is a RPI set, if a positive scalar $\lambda \in \mathbb{R}_{(0,1)}$ exists, such that

$$\begin{aligned}
&\frac{1}{\xi}V_{\#}(\bar{x}^p(\mathcal{F}+1,\kappa)) - \frac{1-\lambda}{\xi}\bar{V}_{\#}(\bar{x}^p(\mathcal{F},\kappa))\\
&\quad \le \frac{\lambda}{\eta^2}\bar{\omega}^{p\mathrm{T}}(\mathcal{F},\kappa)\bar{\omega}^p(\mathcal{F},\kappa)
\end{aligned} \tag{17}$$

where $\bar{V}_{\#}(\bar{x}^p(\mathcal{F},\kappa)) = \max_{\mathcal{G}\in\mathbb{Z}_{\{-d_M,0\}},\bar{b}\in\mathbb{Z}_{\{-b_M,0\}}}\{V_{\#}(\bar{x}^p(\mathcal{F}+\mathcal{G},\kappa+\bar{b})), r(\mathcal{F},\kappa) \in \bar{R}, \bar{\omega}^p(\mathcal{F},\kappa) \in W$. # may denote S or U.

Lemma 2: [31]**:** There are $\varepsilon > 0$ and $\Delta^{pi}(\mathcal{F},\kappa)\Delta^{pi}(\mathcal{F},\kappa) \le I^p$, providing matrixes N^p, $\Delta^p(\mathcal{F},\kappa)$, H^p, and symmetric E, such that

$$E + \varepsilon^{-1}NN^{\mathrm{T}} + \varepsilon H^{p^{\mathrm{T}}}H^p < 0 \tag{18}$$

holds, if

$$E + N^p\Delta^p(\mathcal{F},\kappa)H^p + H^{p^{\mathrm{T}}}\Delta^p(\mathcal{F},\kappa)^{\mathrm{T}}N^{p\mathrm{T}} < 0 \tag{19}$$

Theorem 1: The 2D switching system (13) is stable and the Ω is a RPI set, if a matrix $Y^p \in \mathbb{R}^{n_u^p\times(n_x^p+n_y^p)}$, $Y^{p-1} \in \mathbb{R}^{n_u^{p-1}\times(n_x^{p-1}+n_y^{p-1})}$ matrix $X^p = \mathrm{diag}[X^{ph}, X^{pv}]$, $G^p = \mathrm{diag}[G^{ph}, G^{pv}] > 0$ and a positive scalar $\lambda \in \mathbb{R}_{(0,1)}$ exist, such that the below LMI conditions hold.

$$\begin{bmatrix}
\prod_{0,0} & * & * & * & * & * & *\\
\vdots & \ddots & * & * & * & * & *\\
0 & \cdots & \prod_{d_M,b_M} & * & * & * & *\\
0 & \cdots & 0 & -\frac{\lambda}{\eta^2}I^p & * & * & *\\
\bar{\tilde{A}}_0^p & \cdots & \bar{\tilde{A}}_{-d_M}^p & D & \begin{matrix}-X^p+\varepsilon_1\bar{N}_q^p\bar{N}_q^{p\mathrm{T}}\\ +\varepsilon_2\bar{N}_q^p\bar{N}_q^{p\mathrm{T}}\end{matrix} & * & *\\
\bar{H}_a^pG^p\cdots & \bar{H}_a^pG^p & 0 & 0 & -\varepsilon_1 & * & \\
\bar{H}_b^pY^p\cdots & \bar{H}_b^pY^p & 0 & 0 & 0 & -\varepsilon_1 &
\end{bmatrix} \le 0 \tag{20}$$

Equation (21) shown at the bottom of the next page.

$$\begin{bmatrix} Z & * \\ Y^p & G^p + G^{p\mathrm{T}} - X^p \end{bmatrix} \ge 0, Z_{kk} \le r_{k,\max}^2, k \in Z_{[0,M]} \tag{22}$$

where $\prod_{-\mathcal{G},-\bar{b}} = -\gamma_{\mathcal{G},\bar{b}}(\lambda-1)(G^p + G^{p\mathrm{T}} - X^p)$, $\tilde{\prod}_{-\mathcal{G},-\bar{b}} = -\gamma_{\mathcal{G},\bar{b}}(\lambda-1)(G^{p-1} + G^{(p-1)\mathrm{T}} - X^{p-1}), \mathcal{G} \in \mathbb{Z}_{[-d_M,0]}, \bar{b} \in \mathbb{Z}_{[-b_M,0]}, \bar{\tilde{A}}_j^p = \bar{A}_j^pG^p + \bar{B}^pY^p, j \in \mathbb{Z}_{[-d_M,0]}, P^p = \xi(X^p)^{-1}, F^p = Y^p(G^p)^{-1}, \bar{\tilde{A}}_j^{p-1} = \bar{A}_j^{p-1}G^{p-1} + \bar{B}^{p-1}Y^{p-1}, j \in \mathbb{Z}_{[-d_M,0]}, P^{p-1} = \xi(X^{p-1})^{-1}, \Im = Y^{p-1}(\bar{\boldsymbol{a}}^{p-1})^{-1}$, then Ω is an RPI set. 0and$*$ stand the matrix of order 0 of the appropriate dimensions and the transposition of the corresponding position, respectively.

Proof: Under the match case, the dilation lemma in [32] is adopted, and (23) can be obtained.

$$-G^{p\mathrm{T}}(X^p)^{-1}G^p \le X^p - G^p - G^{p\mathrm{T}} \tag{23}$$

Then, (20) is equivalent to

$$\begin{bmatrix}
\bar{\phi}_{0,0} & * & * & * & * & * & *\\
\vdots & \ddots & * & * & * & * & *\\
0 & \cdots & \bar{\phi}_{d_M,b_M} & * & * & * & *\\
0 & \cdots & 0 & -\frac{\lambda}{\eta^2}I^p & * & * & *\\
\bar{\tilde{A}}_0^p & \cdots & \bar{\tilde{A}}_{-d_M}^p & D & \begin{matrix}-X^p+\varepsilon_1\bar{N}_q^p\bar{N}_q^{p\mathrm{T}}\\ +\varepsilon_2\bar{N}_q^p\bar{N}_q^{p\mathrm{T}}\end{matrix} & * & *\\
\bar{H}_a^pG^p\cdots & \bar{H}_a^pG^p & 0 & 0 & -\varepsilon_1 & * & \\
\bar{H}_b^pY^p\cdots & \bar{H}_b^pY^p & 0 & 0 & 0 & -\varepsilon_2 &
\end{bmatrix} \le 0 \tag{24}$$

where $\bar{\phi}_{-\mathcal{G},-\bar{b}} = -\gamma_{\mathcal{G},\bar{b}}(\lambda-1)(G^{p\mathrm{T}}(X^p)^{-1}G^p)$. By multiplying $\mathrm{diag}[G^{-p\mathrm{T}}, G^{-p\mathrm{T}}, \ldots, G^{-p\mathrm{T}}, I^p, I^p, I^p, I^p]$ and its transpose from both sides of (24), (25) can be obtained.

$$\begin{bmatrix}
\phi_{0,0} & * & * & * & * & * & *\\
\vdots & \ddots & * & * & * & * & *\\
0 & \cdots & \phi_{d_M,b_M} & * & * & * & *\\
0 & \cdots & 0 & -\frac{\lambda}{\eta^2}I^p & * & * & *\\
\bar{A}_0^p & \cdots & \bar{A}_{-d_M}^p & D & \begin{matrix}-X^p+\varepsilon_1\bar{N}_q^p\bar{N}_q^{p\mathrm{T}}\\ +\varepsilon_2\bar{N}_q^p\bar{N}_q^{p\mathrm{T}}\end{matrix} & * & *\\
\bar{H}_a^p & \cdots & \bar{H}_a^p & 0 & 0 & -\varepsilon_1 & *\\
\bar{H}_b^pF^p\cdots & \bar{H}_b^pF^p & 0 & 0 & 0 & -\varepsilon_2 &
\end{bmatrix} \le 0 \tag{25}$$

where $\phi_{-\mathcal{G},-\bar{b}} = -\gamma_{\mathcal{G},\bar{b}}(\lambda-1)(X^p)^{-1}$, $\bar{A}^p_j = \bar{A}^p_j + \bar{B}^p F^p, j \in \mathbb{Z}_{[-d_M,0]}$. By utilizing Schur complement in [33] and Lemma 2, the following inequality can be obtained.

$$\begin{bmatrix} \phi_{0,0} & * & * & * & * \\ \vdots & \ddots & * & * & * \\ 0 & \cdots & \phi_{d_M,b_M} & * & * \\ 0 & \cdots & 0 & -\frac{\lambda}{\eta^2} I^p & * \\ \bar{A}^p_0(\mathcal{F},\kappa) & \cdots & \bar{A}^p_{-d_M}(\mathcal{F},\kappa) & D & -X^p \end{bmatrix} \leq 0 \quad (26)$$

where $\bar{A}^p_j(\mathcal{F},\kappa) = \bar{A}^p_j(\mathcal{F},\kappa) + \bar{B}^p(\mathcal{F},\kappa)F^p, j \in \mathbb{Z}_{[-d_M,0]}$. Further, by utilizing Schur complement lemma, (26) is equivalent to

$$\begin{bmatrix} \phi_{0,0} & * & * & * \\ \vdots & \ddots & * & * \\ 0 & \cdots & \phi_{d_M,b_M} & * \\ 0 & \cdots & 0 & -\frac{\lambda}{\eta^2} I^p \end{bmatrix} + \Upsilon (X^p)^{-1} \Upsilon^{\mathrm{T}} \leq 0 \quad (27)$$

where $\Upsilon = [\tilde{A}^p_0(\mathcal{F},\kappa), \tilde{A}^p_1(\mathcal{F},\kappa), \ldots \tilde{A}^p_{-d_M}(\mathcal{F},\kappa), D]$. Next, by multiplying both left and right sides simultaneously by Φ, we have

$$\Phi \begin{bmatrix} \phi_{0,0} & * & * & * \\ \vdots & \ddots & * & * \\ 0 & \cdots & \phi_{d_M,b_M} & * \\ 0 & \cdots & 0 & -\frac{\lambda}{\eta^2} I^p \end{bmatrix} \Phi^{\mathrm{T}} + \Phi \Upsilon (X^p)^{-1} \Upsilon^{\mathrm{T}} \Phi^{\mathrm{T}} \leq 0 \quad (28)$$

where $\Phi = [\bar{x}^{p\mathrm{T}}(\mathcal{F},\kappa), \bar{x}^{p\mathrm{T}}(\mathcal{F}-1,\kappa-1), \ldots, \bar{x}^{p\mathrm{T}}(\mathcal{F}-d_M,\kappa-b_M), \bar{\omega}^{p\mathrm{T}}(\mathcal{F},\kappa)]$.

Let $(X^p)^{-1} = P^p/\xi$, (28) can be equivalent to

$$\begin{aligned} &(1/\xi)V(\bar{x}^p(\mathcal{F}+1,\kappa)) - (\lambda/\eta^2)\bar{\omega}^{p\mathrm{T}}(\mathcal{F},\kappa)\bar{\omega}^p(\mathcal{F},\kappa) \\ &\leq ((1-\lambda)/\xi)\left(\sum_{\mathcal{G}=-d_M,\bar{b}=b_M}^{0} \gamma_{\mathcal{G},\bar{b}} \bar{V}(\bar{x}^p(\mathcal{F},\kappa))\right) \end{aligned} \quad (29)$$

Considering $\sum_{\mathcal{G}=-d_M,\bar{b}=b_M}^{0} \gamma_{\mathcal{G},\bar{b}} = 1$, $\sum_{\mathcal{G}=-d_M,\bar{b}=b_M}^{0} \gamma_{\mathcal{G},\bar{b}} \bar{V}(\bar{x}^p(\mathcal{F}+\mathcal{G},\kappa+\bar{b})) \leq \bar{V}(\bar{x}^p(\mathcal{F},\kappa))$ can be easily obtained. Obviously, (17) can be obtained. Like the match case, the proof of the mismatch case is omitted. Moreover, (22) is utilized to guarantee the input constraint. According to Definition 1, we have

$$\begin{aligned} ||r^p(\mathcal{F},\kappa)|| &= ||F^P \bar{x}^p(\mathcal{F},\kappa)|| = \bar{x}^{p\mathrm{T}}(\mathcal{F},\kappa)F^{p\mathrm{T}}F^p\bar{x}^p(\mathcal{F},\kappa) \\ &= \bar{x}^{p\mathrm{T}}(\mathcal{F},\kappa)(Y^p(G^p)^{-1})^{\mathrm{T}}Y^p(G^p)^{-1}\bar{x}^p(\mathcal{F},\kappa) \\ &= \bar{x}^{p\mathrm{T}}(\mathcal{F},\kappa)(Y^p(G^p)^{-1})^{\mathrm{T}}(X^p)^{-1}X^pY^p(G^p)^{-1}\bar{x}^p(\mathcal{F},\kappa) \\ &\leq (G^{p^{\mathrm{T}}})^{-1}Y^{p\mathrm{T}}X^pY^p(G^p)^{-1} \leq -Y^{p\mathrm{T}}(X^p - G^{p\mathrm{T}} - G^p)Y^p \\ &\leq (r^p)^2_{\max} \end{aligned} \quad (30)$$

Clearly, (22) is got by utilizing Schur complement lemma. Proof 1 is completed.

Terminal constraint set:

Definition 2: For the terminal constraint set Ω_V, there are two necessary conditions. First, it is an RPI set. Second, $\vartheta_1, \vartheta_2 \in \kappa_\infty$, positive definite function $V(\bar{x}^p(\mathcal{F}+\zeta|\mathcal{F},\kappa+k|\kappa))$ existed and satisfied

$$\begin{aligned} &\vartheta_1(||\bar{x}^p(\mathcal{F}+\zeta,\kappa+k)||) \leq V(\bar{x}^p(\mathcal{F}+\zeta,\kappa+k) \\ &\quad \leq \vartheta_2(||\bar{x}^p(\mathcal{F}+\zeta,\kappa+k||) \end{aligned} \quad (31)$$

$$\begin{aligned} &V(\bar{x}^p(\mathcal{F}+1+\zeta,\kappa+k)) - \varsigma^{p\#}V(\bar{x}^p(\mathcal{F}+\zeta,\kappa+k)) \\ &\quad = V_S^h(\bar{x}^p(\mathcal{F}+1+\zeta,\kappa+k)) - \varsigma^{p\#1}V_S^h(\bar{x}^p(\mathcal{F}+\zeta,\kappa+k)) \\ &\qquad + V_S^v(\bar{x}^p(\mathcal{F}+\zeta,\kappa+k)) - \varsigma^{p\#2}V_S^v(\bar{x}^p(\mathcal{F}+\zeta,\kappa+k)) \\ &\quad \leq -\bar{x}^{p\mathrm{T}}(\mathcal{F}+\zeta,\kappa+k)Q^p\bar{x}^p(\mathcal{F}+\zeta,\kappa+k) - r^{p^{\mathrm{T}}}(\mathcal{F}+\zeta,\kappa+k) \\ &\qquad R^p r^p(\mathcal{F}+\zeta,\kappa+k) + \tau\bar{\omega}^{p\mathrm{T}}(\mathcal{F}+\zeta,\kappa+k)\bar{\omega}^p(\mathcal{F}+\zeta,\kappa+k) \end{aligned} \quad (32)$$

where $\varsigma^{p\#} = \max\{\varsigma^{p\#1}, \varsigma^{p\#2}\}$ denote the system decay coefficient, $\# \in \{S,U\}$.

Theorem 2: Considering (14), if Theorem 1 is true, the below inequalities are feasible

$$\begin{bmatrix} \Lambda^p & * & * & * & * \\ \mathbb{C}^p & -\varepsilon_1 & * & * & * \\ \mathbb{Q}^p & 0 & -\varepsilon_2 & * & * \\ Q^pG^p & 0 & 0 & -\xi Q^p & * \\ R^pY^p & 0 & 0 & 0 & -\xi R^p \end{bmatrix} \leq 0 \quad (33)$$

$$\begin{bmatrix} \Lambda^{p-1} & * & * & * & * \\ \mathbb{C}^{p-1} & -\varepsilon_1 & * & * & * \\ \mathbb{Q}^{p-1} & 0 & -\varepsilon_2 & * & * \\ Q^{p-1}G^{p-1} & 0 & 0 & -\xi Q^{p-1} & * \\ R^{p-1}\Im & 0 & 0 & 0 & -\xi R^{p-1} \end{bmatrix} \leq 0 \quad (34)$$

$$\begin{bmatrix} \tilde{\Pi}_{0,0} & * & * & * & * & * & * \\ \vdots & \ddots & * & * & * & * & * \\ 0 & \cdots & \tilde{\Pi}_{d_M,b_M} & * & * & * & * \\ 0 & \cdots & 0 & -\frac{\lambda}{\eta^2} I^{p-1} & * & * & * \\ \bar{\tilde{A}}^p_0 & \cdots & \bar{\tilde{A}}^p_{-d_M} & D & \begin{matrix} -X^{p-1} + \varepsilon_1 \bar{N}_q^{p-1} \bar{N}_q^{(p-1)\mathrm{T}} \\ + \varepsilon_2 \bar{N}_q^{p-1} \bar{N}_q^{(p-1)\mathrm{T}} \end{matrix} & * & * \\ \bar{H}^p_a G^{p-1} & \cdots & \bar{H}^p_a G^{p-1} & 0 & 0 & -\varepsilon_1 & * \\ \bar{H}^p_b \Im & \cdots & \bar{H}^p_b \Im & 0 & 0 & 0 & -\varepsilon_2 \end{bmatrix} \leq 0 \quad (21)$$

$$\begin{bmatrix} 1 & \bar{x}^{p\mathrm{T}}(\mathcal{F}+\mathcal{G},\kappa+\bar{b}) \\ \bar{x}^{p}(\mathcal{F}+\mathcal{G},\kappa+\bar{b}) & X^{p} \end{bmatrix} \geq 0, \quad \begin{matrix} \mathcal{G}\in\mathbb{Z}_{[-d_M,0]}, \\ \bar{b}\in\mathbb{Z}_{[-b_M,0]} \end{matrix} \tag{35}$$

where

$$\Lambda^{p}=\begin{bmatrix} \widehat{\prod}_{0,0} & * & * & * & * \\ \vdots & \ddots & * & * & * \\ 0 & \cdots & \widehat{\prod}_{d_M,b_M} & * & * \\ 0 & \cdots & 0 & -\tau\xi I^{p} & * \\ \bar{\tilde{A}}_{0}^{p} & \cdots & \bar{\tilde{A}}_{-d_M}^{p} & D & \begin{matrix} -X^{p}+\varepsilon_1\bar{N}_{q}^{p}\bar{N}_{q}^{p\mathrm{T}} \\ +\varepsilon_2\bar{N}_{q}^{p}\bar{N}_{q}^{p\mathrm{T}} \end{matrix} \end{bmatrix},$$

$$\Lambda^{p-1}=\begin{bmatrix} \hat{\prod}_{0,0} & * & * & * \\ \vdots & \ddots & * & * \\ 0 & \cdots & \hat{\prod}_{d_M,b_M} & * \\ 0 & \cdots & 0 & -\tau\xi I^{p-1} \\ \bar{\tilde{A}}_{0}^{p-1} & \cdots & \bar{\tilde{A}}_{-d_M}^{p-1} & D \end{bmatrix}$$

$$\begin{bmatrix} * \\ * \\ * \\ * \\ -X^{p-1}+\varepsilon_1\bar{N}_{q}^{p-1}\bar{N}_{q}^{(p-1)\mathrm{T}}+\varepsilon_2\bar{N}_{q}^{p-1}\bar{N}_{q}^{(p-1)\mathrm{T}} \end{bmatrix},$$

$$\widehat{\prod}_{-\mathcal{G},-\bar{b}}=-\varsigma^{pS}\gamma_{\mathcal{G},\bar{b}}(G^{p}+G^{p\mathrm{T}}-X^{p}),$$

$$\hat{\prod}_{-\mathcal{G},-\bar{b}}=-\varsigma^{pU}\gamma_{\mathcal{G},\bar{b}}(G^{p-1}+G^{(p-1)\mathrm{T}}-X^{p-1}),$$

$$\mathcal{G}\in\mathbb{Z}_{[-d_M,0]},\bar{b}\in\mathbb{Z}_{[-b_M,0]},$$

$$\mathbb{C}^{p}=[\bar{H}_{a}^{p}G^{p},\ldots,\bar{H}_{a}^{p}G^{p},0,0],$$

$$\mathbb{Q}^{p}=[\bar{H}_{b}^{p}Y^{p},\ldots,\bar{H}_{b}^{p}Y^{p},0,0,0],$$

$$\mathbb{C}^{p-1}=[\bar{H}_{a}^{p}G^{p-1},\ldots,\bar{H}_{a}^{p}G^{p-1},0,0],$$

$$\mathbb{Q}^{p-1}=[\bar{H}_{b}^{p}\Im,\ldots,\bar{H}_{a}^{p}\Im,0,0,0],$$

$$\bar{\tilde{A}}_{j}^{p}=\bar{A}_{j}^{p}G^{p}+\bar{B}^{p}Y^{p},j\in\mathbb{Z}_{[-d_M,0]},$$

$$P^{p}=\xi(X^{p})^{-1},F^{p}=Y^{p}(G^{p})^{-1},$$

$$\bar{\tilde{A}}_{j}^{p-1}=\bar{A}_{j}^{p}G^{p-1}+\bar{B}^{p}Y^{p-1},j\in\mathbb{Z}_{[-d_M,0]},$$

$$P^{p-1}=\xi(X^{p-1})^{-1},\Im=F^{p-1}(\bar{\boldsymbol{a}}^{p-1})^{-1},$$

then Ω_V is a terminal constraint set.

Proof: First, by solving the characteristic value, we can easily obtain.

$$\begin{aligned}\bar{\rho}_{\min}||\bar{x}^{p}(\mathcal{F}+\zeta,\kappa+k)||^{2}&\leq V(\bar{x}^{p}(\mathcal{F}+\zeta,\kappa+k)\\&\leq\bar{\rho}_{\max}||\bar{x}^{p}(\mathcal{F}+\zeta,\kappa+k||^{2}\end{aligned}\tag{36}$$

where $\bar{\rho}_{\min}:=\min\{\rho_{\min}(P)\}$, $\bar{\rho}_{\max}:=\min\{\rho_{\max}(P)\}$. $\rho_{\min}(\cdot)$ and $\rho_{\max}(\cdot)$ respectively is the maximal and minimal eigenvalues.

Under the match case, for (33), by multiplying both left and right sides by $\mathrm{diag}[G^{-p\mathrm{T}},G^{-p\mathrm{T}},\ldots,G^{-p\mathrm{T}},I^{p},I^{p},I^{p},I^{p},I^{p},I^{p}]$, we obtained

$$\begin{bmatrix} \bar{\Lambda}^{p} & * & * & * & * \\ \bar{\mathbb{C}}^{p} & -\varepsilon_1 & * & * & * \\ \bar{\mathbb{Q}}^{p} & 0 & -\varepsilon_2 & * & * \\ Q^{p} & 0 & 0 & -\xi Q^{p} & * \\ R^{p}F^{p} & 0 & 0 & 0 & -\xi R^{p} \end{bmatrix}\leq 0 \tag{37}$$

where

$$\bar{\Lambda}^{p}=\begin{bmatrix} \bar{\coprod}_{0,0} & * & * & * & * \\ \vdots & \ddots & * & * & * \\ 0 & \cdots & \bar{\coprod}_{d_M,b_M} & * & * \\ 0 & \cdots & 0 & -\tau\xi I^{p} & * \\ \bar{A}_{0}^{p} & \cdots & \bar{A}_{d_M}^{p} & D & \begin{matrix} -X^{p}+\varepsilon_1\bar{N}_{q}^{p}\bar{N}_{q}^{p\mathrm{T}} \\ +\varepsilon_2\bar{N}_{q}^{p}\bar{N}_{q}^{p\mathrm{T}} \end{matrix} \end{bmatrix},$$

$$\bar{\mathbb{C}}^{p}=[\bar{H}_{a}^{p},\ldots,\bar{H}_{a}^{p},0,0],\bar{\mathbb{Q}}^{p}=[\bar{H}_{b}^{p},\ldots,\bar{H}_{b}^{p},0,0,0],$$

$\bar{\coprod}_{d_M,b_M}=-\varsigma^{pS}\gamma_{\mathcal{G},\bar{b}}(X^{p})^{-1}$. And the below inequality is obtained by utilizing Schur complement and Lemma 2.

$$\begin{bmatrix} \bar{\coprod}_{0,0} & * & * & * & * & * & * \\ \vdots & \ddots & * & * & * & * & * \\ 0 & \cdots & \bar{\coprod}_{d_M,b_M} & * & * & * & * \\ 0 & \cdots & 0 & -\tau\xi I^{p} & * & * & * \\ \bar{A}_{0}^{p}(\mathcal{F},\kappa) & \cdots & \bar{A}_{-d_M}^{p}(\mathcal{F},\kappa) & D & -X^{p} & * & * \\ Q^{p} & \cdots & 0 & 0 & 0 & -\xi Q^{p} & * \\ R^{p}F^{p} & \cdots & 0 & 0 & 0 & 0 & -\xi R^{p} \end{bmatrix}\leq 0 \tag{38}$$

where $\bar{A}_{j}^{p}(\mathcal{F},\kappa)=\bar{A}_{j}^{p}(\mathcal{F},\kappa)+\bar{B}^{p}(\mathcal{F},\kappa)F^{p},j\in\mathbb{Z}_{[-d_M,0]}$.

Then, (38) can be rewritten as

$$\begin{bmatrix} \bar{\coprod}_{0,0} & * & * & * & * & * & * \\ \vdots & \ddots & * & * & * & * & * \\ 0 & \cdots & \bar{\coprod}_{d_M,b_M} & * & * & * & * \\ 0 & \cdots & 0 & -\tau I^{p} & * & * & * \\ \bar{A}_{0}^{p}(\mathcal{F},\kappa) & \cdots & \bar{A}_{-d_M}^{p}(\mathcal{F},\kappa) & D & -\frac{X^{p}}{\xi} & * & * \\ Q^{p} & \cdots & 0 & 0 & 0 & -Q^{p} & * \\ R^{p}F^{p} & \cdots & 0 & 0 & 0 & 0 & -R^{p} \end{bmatrix}\leq 0 \tag{39}$$

where $\bar{\coprod}_{d_M,b_M}=-\varsigma^{pS}\gamma_{\mathcal{G},\bar{b}}\xi(X^{p})^{-1}$. Further, let $(X^{p})^{-1}=P^{p}/\xi$, (39) is transformed by Schur complement (40) shown at the bottom of the next page, where $\mho=Q^{p}+F^{p\mathrm{T}}R^{p}F^{p}-\varsigma^{pS}\gamma_{0,0}P^{p}$. By utilizing Schur complement and multiplying both left and right sides by $[\bar{x}^{p\mathrm{T}}(\mathcal{F}+\zeta,\kappa+k),\bar{x}^{p\mathrm{T}}(\mathcal{F}-1+\zeta,\kappa-1+k),\ldots,\bar{x}^{p\mathrm{T}}(\mathcal{F}-d_M+l,\kappa-b_M+k),\ \bar{\omega}^{p\mathrm{T}}(\mathcal{F}+\zeta,\kappa+$

$k)]^{\mathrm{T}}$, (39) can be easily obtained.

$$\begin{aligned}
&\left(\begin{array}{c}\sum_{\mathcal{G}=-d_M,\bar{b}=-b_M}^{0}\bar{A}_g^p(\mathcal{F},\kappa)\bar{x}^p(\mathcal{F}+\mathcal{G}+\zeta,\kappa+\bar{b}+k)\\ +\bar{B}^p(\mathcal{F},\kappa)r^p(\mathcal{F}+\zeta,\kappa+k)\\ +D\bar{\omega}^p(\mathcal{F}+\zeta,\kappa+k)\end{array}\right)^{\mathrm{T}}\\
&P^p\left(\begin{array}{c}\sum_{\mathcal{G}=-d_M,\bar{b}=-b_M}^{0}\bar{A}_g^p(\mathcal{F},\kappa)\bar{x}^p(\mathcal{F}+g,\kappa+\bar{b})\\ +\bar{B}^p(\mathcal{F},\kappa)r^p(\mathcal{F}+\zeta,\kappa+k)\\ +D\bar{\omega}^p(\mathcal{F}+\zeta,\kappa+k)\end{array}\right)\\
&+\bar{x}^{p\mathrm{T}}(\mathcal{F}+\zeta,\kappa+k)Q^p\bar{x}^p(\mathcal{F}+\zeta,\kappa+k)+\bar{x}^{p\mathrm{T}}(\mathcal{F}+\zeta,\kappa+k)\\
&F^{p\mathrm{T}}R^pF^p\bar{x}^p(\mathcal{F}+\zeta,\kappa+k)-\varsigma^{pS}\sum_{\mathcal{G}=-d_M,\bar{b}=-b_M}^{0}\\
&\times\gamma_{g,\bar{b}}\bar{x}^{p\mathrm{T}}(\mathcal{F}+\mathcal{G}+\zeta,\kappa+\bar{b}+k)P^p\\
&\bar{x}^p(\mathcal{F}+\mathcal{G}+\zeta,\kappa+\bar{b}+k)-\tau\bar{\omega}^{p\mathrm{T}}(\mathcal{F}+\zeta,\kappa+k)\bar{\omega}^p(\mathcal{F}+\zeta,\kappa+k)\le 0
\end{aligned}\tag{41}$$

Because of $\sum_{\mathcal{G}=-d_M,\bar{b}=b_M}^{0}\gamma_{\mathcal{G},\bar{b}}=1$, it has $\sum_{\mathcal{G}=-d_M,\bar{b}=b_M}^{0}\gamma_{\mathcal{G},\bar{b}}\ \bar{V}(\bar{x}^p(\mathcal{F}+\zeta|\mathcal{F},\kappa+k|\kappa))\le\bar{V}(\bar{x}^p(\mathcal{F}+\zeta|\mathcal{F},\kappa+\mathcal{G}|\kappa))$.

Therefore, the following equation can be established under the match case.

$$\begin{aligned}
&V(\bar{x}^p(\mathcal{F}+1+\mathcal{G}|\mathcal{F},\kappa+\bar{b}|\kappa))-\varsigma^{pS}V(\bar{x}^p(\mathcal{F}+\mathcal{G}|\mathcal{F},\kappa+\bar{b}|\kappa))\\
&\quad=V_S^h(\bar{x}^p(\mathcal{F}+1+\mathcal{G}|\mathcal{F},\kappa+\bar{b}|\kappa))\\
&\qquad-\varsigma^{pS1}V_S^h(\bar{x}^p(\mathcal{F}+\mathcal{G}|\mathcal{F},\kappa+\bar{b}|\kappa))\\
&\qquad+V_S^v(\bar{x}^p(\mathcal{F}+\mathcal{G}|\mathcal{F},\kappa+1+\bar{b}|\kappa))\\
&\qquad-\varsigma^{pS2}V_S^v(\bar{x}^p(\mathcal{F}+\mathcal{G}|\mathcal{F},\kappa+\bar{b}|\kappa))\\
&\quad\le-\bar{x}^{p\mathrm{T}}(\mathcal{F}+\mathcal{G}|\mathcal{F},\kappa+\bar{b}|\kappa)Q^p\bar{x}^p(\mathcal{F}+\mathcal{G}|\mathcal{F},\kappa+\bar{b}|\kappa)\\
&\qquad-r^{p^{\mathrm{T}}}(\mathcal{F}+\mathcal{G}|\mathcal{F},\kappa+\bar{b}|\kappa)R^pr^p(\mathcal{F}+\mathcal{G}|\mathcal{F},\kappa+\bar{b}|\kappa)\\
&\qquad+\tau\bar{\omega}^{p\mathrm{T}}(\mathcal{F}+\mathcal{G}|\mathcal{F},\kappa+\bar{b}|\kappa)\bar{\omega}^p(\mathcal{F}+\mathcal{G}|\mathcal{F},\kappa+\bar{b}|\kappa)
\end{aligned}\tag{42}$$

where $\varsigma^{pS}=\max\{\varsigma^{pS1},\ \varsigma^{pS2}\}$ denote the system decay coefficient under the match case.

Like the match case, under the mismatch case, (44) can be clearly obtained.

$$\begin{aligned}
&V(\bar{x}^p(\mathcal{F}+1+\mathcal{G}|\mathcal{F},\kappa+\bar{b}|\kappa))-\varsigma^{pU}V(\bar{x}^p(\mathcal{F}+\mathcal{G}|\mathcal{F},\kappa+\bar{b}|\kappa))\\
&\quad=V_U^h(\bar{x}^p(\mathcal{F}+1+\mathcal{G}|\mathcal{F},\kappa+\bar{b}|\kappa))\\
&\qquad-\varsigma^{pU1}V_U^h(\bar{x}^p(\mathcal{F}+\mathcal{G}|\mathcal{F},\kappa+\bar{b}|\kappa))\\
&\qquad+V_U^v(\bar{x}^p(\mathcal{F}+\mathcal{G}|\mathcal{F},\kappa+1+\bar{b}|\kappa))\\
&\qquad-\varsigma^{pU2}V_S^v(\bar{x}^p(\mathcal{F}+\mathcal{G}|\mathcal{F},\kappa+\bar{b}|\kappa))\\
&\quad\le-\bar{x}^{p\mathrm{T}}(\mathcal{F}+\mathcal{G}|\mathcal{F},\kappa+\bar{b}|\kappa)Q^p\bar{x}^p(\mathcal{F}+\mathcal{G}|\mathcal{F},\kappa+\bar{b}|\kappa)\\
&\qquad-r^{p^{\mathrm{T}}}(\mathcal{F}+\mathcal{G}|\mathcal{F},\kappa+\bar{b}|\kappa)R^pr^p(\mathcal{F}+\mathcal{G}|\mathcal{F},\kappa+\bar{b}|\kappa)\\
&\qquad+\tau\bar{\omega}^{p\mathrm{T}}(\mathcal{F}+\mathcal{G}|\mathcal{F},\kappa+\bar{b}|\kappa)\bar{\omega}^p(\mathcal{F}+\mathcal{G}|\mathcal{F},\kappa+\bar{b}|\kappa)
\end{aligned}\tag{43}$$

where $\varsigma^{pU}=\max\{\varsigma^{pU1},\varsigma^{pU2}\}$ denotes the system decay coefficient under the mismatch case. Therefore, (32) is satisfied.

Considering the RPI properties, the terminal constraint set Ω_V, i.e., $\bar{x}^p(\mathcal{F}+\mathcal{G},\kappa+\bar{b})\in\Omega_V,\mathcal{G}\in\mathbb{Z}_{[-d_M,0]},\bar{b}\in\mathbb{Z}_{[-b_M,0]}$, meets the below condition.

$$V(\bar{x}^p(\mathcal{F},\kappa))\le\xi\tag{44}$$

yet

$$\bar{x}^{p\mathrm{T}}(\mathcal{F}+\mathcal{G},\kappa+\bar{b})P^p\bar{x}^p(\mathcal{F}+\mathcal{G},\kappa+\bar{b})\le\xi\tag{45}$$

Let $X^p=\xi(P^p)^{-1}$, we can easily obtain (35).

To this end, Theorem 2 is proved.

Remark 3: As is obvious, the dimensionality of LMI obtained by LRF-based methods is influenced by the time delay. The larger the time delay, the larger the dimensionality of the stability condition in the form of LMI, which in turn leads to an increase in the computational effort and conservativeness of the LMI condition. In other words, the smaller the time delay, the LMI conditions will be less computationally intensive and less conservative. In contrast, the LKF method is a redesign of the Lyapunov function using information on the upper and lower bounds of the time delay. The conservativeness and computational effort are derived from a large number of unknown matrices present in the Lyapunov function, and the dimensionality of LMI is independent of the time delay ranges. Generally, for small-delay batch processes, the computational effort of the LRF-based method is significantly lower than the LKF-based method.

Stability analysis: The system's exponential stability analysis is provided, the Max-RT and Min-RT are solved.

Theorem 3: The 2D system (13) is exponentially stable, when the Lyapunov function $V_{\#}^p(\bar{x}^p(\mathcal{F},\kappa))$, the Max-DT and the Min-DT meet the following conditions.

$$\begin{cases}V_S^p(\bar{x}^p(\mathcal{F},\kappa))\le\mu_p^SV_S^{p-1}(\bar{x}^p(\mathcal{F},\kappa))\\ V_S^p(\bar{x}^p(\mathcal{F},\kappa))\le\mu_p^SV_U^p(\bar{x}^p(\mathcal{F},\kappa))\\ V_U^p(\bar{x}^p(\mathcal{F},\kappa))\le\mu_p^UV_S^{p-1}(\bar{x}^p(\mathcal{F},\kappa))\end{cases}\tag{46}$$

$$\mathfrak{M}_S^p\ge-\frac{\ln\mu_p^S}{\ln\varsigma_p^S},\mathfrak{M}_U^p\le-\frac{\ln\mu_p^U}{\ln\varsigma_p^U}\tag{47}$$

where $\mu_\rho^S>1,0<\mu_\rho^U<1$.

Proof: Under the match case, based on (42), we can obtain the below equation.

$$\begin{aligned}
&V(\bar{x}^p(\mathcal{F}+1+\mathcal{G}|\mathcal{F},\kappa+\bar{b}|\kappa))-\varsigma^{pS}V(\bar{x}^p(\mathcal{F}+\mathcal{G}|\mathcal{F},\kappa+\bar{b}|\kappa))\\
&\quad\le-\bar{x}^{p\mathrm{T}}(\mathcal{F}+\mathcal{G}|\mathcal{F},\kappa+\bar{b}|\kappa)Q^p\bar{x}^p(\mathcal{F}+\mathcal{G}|\mathcal{F},\kappa+\bar{b}|\kappa)
\end{aligned}$$

$$\begin{bmatrix}
\mho & * & * & * & * & *\\
0 & -\gamma_{-1,-1}\varsigma^{pS}P^p & * & * & * & *\\
\vdots & \vdots & \ddots & * & * & *\\
0 & 0 & \cdots & -\gamma_{-d_M,-\bar{b}_M}\varsigma^{pS}P^p & * & *\\
0 & 0 & \cdots & 0 & -\tau I^p & *\\
\bar{A}_0^p(\mathcal{F},\kappa) & \bar{A}_{-1}^p(\mathcal{F},\kappa) & \cdots & \bar{A}_{-d_M}^p(\mathcal{F},\kappa) & D & -(P^p)^{-1}
\end{bmatrix}\le 0\tag{40}$$

$$-r^{p^{\mathrm{T}}}(\mathcal{F}+\mathcal{G}\mathcal{F},\kappa+\bar{b}|\kappa)R^{p}r^{p}(\mathcal{F}+\mathcal{G}|\mathcal{F},\kappa+\bar{b}|\kappa)$$
$$+\tau\bar{\omega}^{p\mathrm{T}}(\mathcal{F}+\mathcal{G}|\mathcal{F},\kappa+\bar{b}|\kappa)\bar{\omega}^{p}(\mathcal{F}+\mathcal{G}|\mathcal{F},\kappa+\bar{b}|\kappa)\leq 0 \tag{48}$$

Based on (48), we have

$$V(\bar{x}^{p}(\mathcal{F}+1+\zeta|\mathcal{F},\kappa+k))\leq\varsigma^{pS}V(\bar{x}^{p}(\mathcal{F}+\zeta|\mathcal{F},\kappa+k)) \tag{49}$$

By accumulating both sides of (49) from $\zeta,k=0$ to ∞, (50) can be easily obtained.

$$\sum_{\mathcal{F}+\kappa=\zeta+k+1}V(\bar{x}^{p}(\mathcal{F},\kappa))<\varsigma^{pS}\sum_{\mathcal{F}+\kappa=\zeta+k}V(\bar{x}^{p}(\mathcal{F},\kappa)) \tag{50}$$

According to the switching sequence (5), we define $\grave{\lambda}_{k}^{pS}=\mathcal{F}_{\bar{k}}^{pS}+\kappa_{\bar{k}}$ and $\grave{\lambda}_{\bar{k}}^{pU}=\mathcal{F}_{\bar{k}}^{pU}+\kappa_{\bar{k}}$, where $\grave{\lambda}_{k}^{pS}$ and $\grave{\lambda}_{\bar{k}}^{pU}$ represent the total number of rolls within batches under the match and mismatch cases, and $\bar{\kappa}=1,2,\ldots\kappa$. $V^{p}_{(\bar{\mathcal{F}}^{pS},K_k)}(\bar{x}^{p}(\mathcal{F},\kappa))$ and $V^{p}_{\ell(\bar{\mathcal{F}}^{pU},k_k)}(\bar{x}^{p}(\mathcal{F},\kappa)$ represent the Lyapunov function of phase p with the match and mismatch cases. $N_{\Gamma}^{pS}(d,O)$ and $\bar{\mathcal{F}}^{pS}(d,O)$ are the switching numbers and the total running time of all batches, respectively. For any $\mathcal{F}+\kappa=O\geq d$, in an interval time $[d,O]$, we have

$$\sum_{\mathcal{F}+\kappa=O}V^{p}_{(\bar{\mathcal{F}}^{pS},\kappa_k)}(\bar{x}^{p}(\mathcal{F},\kappa))<\left(\varsigma^{pS}\right)^{O-\hbar_{k}^{pS}}\sum_{\mathcal{F}+\kappa=\grave{\lambda}_{k}^{pS}}$$
$$\times V^{p}_{(\bar{\mathcal{F}}^{pS},\kappa_k)}(\bar{x}^{p}(\mathcal{F},\kappa)) \tag{51}$$

Considering conditions (46), at the switching point, (52) holds.

$$\sum_{\mathcal{F}+\kappa=\grave{\lambda}_{k}^{pU}}V^{p}_{\ell(\bar{\mathcal{F}}^{pS},\kappa_k)}(\bar{x}^{p}(\mathcal{F},\kappa))<\mu^{pU}\sum_{\mathcal{F}+\kappa=\grave{\lambda}_{k}^{pU}}$$
$$\times V^{p}_{\ell(\bar{\mathcal{F}}^{pU},\kappa_k)}(\bar{x}^{p}(\mathcal{F},\kappa)) \tag{52}$$

Then, combine (51) and (52), we have

$$\sum_{\mathcal{F}+\kappa=O}V^{p}_{(\bar{\mathcal{F}}^{pS},k_k)}(\bar{x}^{p}(\mathcal{F}+\kappa))<\left(\varsigma^{pS}\right)^{O-\hbar_{k}^{pS}}$$
$$\times\sum_{\mathcal{F}+\kappa=\grave{\lambda}_{k}^{pS}}V^{p}_{(\bar{\mathcal{F}}^{pS},k_k)}(\bar{x}^{p}(\mathcal{F},\kappa))$$
$$\leq\mu^{pS}\left(\varsigma^{pS}\right)^{O-\grave{\lambda}_{k}^{pS}}\sum_{\mathcal{F},\kappa=\grave{\lambda}_{k}^{pS}}V^{p}_{\ell(\bar{\mathcal{F}}^{pU},k_k)}(\bar{x}^{p}(\mathcal{F},\kappa))$$
$$\leq\left(\varsigma^{pS}\right)^{O-\grave{\lambda}_{k}^{pS}}\mu^{pS}\left(\varsigma^{pU}\right)^{\grave{\lambda}_{k}^{pS}-\grave{\lambda}_{k}^{pU}}\sum_{\mathcal{F}+\kappa=\hbar_{k}^{pU}}V^{p}_{\ell(\bar{\mathcal{F}}^{pU},k_k)}(\bar{x}^{p}(\mathcal{F},\kappa))$$
$$\leq\left(\varsigma^{pS}\right)^{O-\grave{\lambda}_{k}^{pS}}\mu^{pS}\left(\varsigma^{pU}\right)^{\grave{\lambda}_{k}^{pS}-\grave{\lambda}_{k}^{pU}}\mu^{pU}$$
$$\times\sum_{\mathcal{F}+\kappa=\grave{\lambda}_{k}^{pU}}V^{p}_{\ell(\bar{\mathcal{F}}^{pU},k_k)}(\bar{x}^{p}(\mathcal{F},\kappa))$$
$$\vdots$$
$$\leq\prod_{p=1}^{p}\left(\mu^{pS}\right)^{N_0^{p}+\left(\bar{\mathcal{F}}_{S}^{p}(d,O)/\mathfrak{M}_{S}^{\rho}\right)}\times\prod_{p=1}^{p}\left(\varsigma^{pS}\right)^{\bar{\mathcal{F}}^{pS}(d,O)}$$
$$\times\prod_{p=1}^{p}\left(\varsigma^{pU}\right)^{N_0^{U}+\left(\bar{\mathcal{F}}_{U}^{\rho}(d,O)/\mathfrak{M}_{U}^{\rho}\right)}$$
$$\times\prod_{p=1}^{p}\left(\varsigma^{pS}\right)^{\bar{\mathcal{F}}^{pU}(d,O)}\times\sum_{\mathcal{F}+\kappa=d}V^{p}_{\ell(\bar{\mathcal{F}}^{2U},k_k)}(\bar{x}^{p}(\mathcal{F},\kappa))=\exp$$
$$\left(\sum_{p=1}^{p}N_0^{S}\ln\mu^{pS}+\sum_{p=1}^{p}N_0^{U}\ln\mu^{pU}\right)$$
$$\times\prod_{p=1}^{p}\left(\left(\mu^{pS}\right)^{1/\mathfrak{M}_{S}^{p}}(\varsigma^{pS})\right)^{\bar{\mathcal{F}}^{\rho S}(d,O)}$$
$$\times\prod_{p=1}^{p}\left(\left(\mu^{pU}\right)^{1/\mathfrak{M}_{U}^{p}}(\varsigma^{pU})\right)^{\bar{\mathcal{F}}^{pU}(d,O)}$$
$$\times\sum_{T+K=d}\boldsymbol{v}^{p}_{\ell(\bar{\mathcal{F}}^{2U},k_k)}(\bar{x}^{p}(\mathcal{F},\kappa)) \tag{53}$$

From (47), and considering $0<\varsigma^{pS}<1,\varsigma^{pU}>1,\mu^{pS}>1$, $0<\mu^{pU}<1$, it has

$$\begin{cases}\mathfrak{M}_{S}^{p}\ln\varsigma^{pS}+\ln\mu^{pS}\leq 0\\ \mathfrak{M}_{U}^{p}\ln\varsigma^{pU}+\ln\mu^{pU}\leq 0\end{cases} \tag{54}$$

yet

$$\begin{cases}\left(\mu^{pS}\right)^{1/\mathfrak{M}_{S}^{\rho}}(\varsigma^{pS})=\exp\left(\left[1/\mathfrak{M}_{S}^{\rho}\ln\mu^{pS}+\ln\varsigma^{pS}\right]\right)\\ \left(\mu^{pU}\right)^{1/\mathfrak{M}_{U}^{\rho}}(\varsigma^{pU})=\exp\left(\left[1/\mathfrak{M}_{U}^{\rho}\ln\mu^{pU}+\ln\varsigma^{pU}\right]\right)\end{cases} \tag{55}$$

Let $\Gamma=\max((\mu^{pS})^{1/\mathfrak{M}_{S}^{p}}(\varsigma^{pS}),(\mu^{pU})^{1/\mathfrak{M}_{U}^{p}}(\varsigma^{pU}))$, $\upsilon=\exp(\sum_{\mathrm{p}=1}^{\mathrm{p}}\mathrm{N}_0^{\mathrm{S}}\ln\mu^{\mathrm{pS}}+\sum_{p=1}^{p}N_0^{U}\ln\mu^{pU})$, we have

$$\sum_{\mathcal{F}+\kappa=O}V^{p}_{\ell(\bar{\mathcal{F}}^{pS},k_k)}(\bar{x}^{p}(\mathcal{F},\kappa))\leq\upsilon\Gamma^{O-d}$$
$$\times\sum_{\mathcal{F}+\kappa=d}V^{p}_{\ell(\bar{\mathcal{F}}^{pU},k_k)}(\bar{x}^{p}(\mathcal{F},\kappa)) \tag{56}$$

Therefore, $V^{p}_{\ell(\bar{\mathcal{F}}^{pS},K_k)}(\bar{x}^{p}(\mathcal{F},\kappa))$ is convergent with marginal Γ if the switching signals satisfy (47). Proof 3 is completed.

D. ILHRPC Algorithm Steps

Step 1: The complete system state $\bar{x}^{p}(\mathcal{F}+\mathcal{G},\kappa+\bar{b})$, $\mathcal{G}\in\mathbb{Z}_{[-d_M,-1]},\bar{b}\in\mathbb{Z}_{[-b_M,-1]}$ is obtained.

Step 2: In any batch $\mathcal{F}$ at the time κ, the below optimization problem is:

$$\begin{aligned}&\min\nolimits_{\xi,Y^{p},Y^{p-1},G^{p},Z^{p},X^{p},\lambda}\xi\\&\text{subject to (20), (21), (22), (33), (34) and (35)}\end{aligned} \tag{57}$$

The ILHRPC law under the match case $r^{p}(\mathcal{F},\kappa)=F^{p}\bar{x}^{p}(\mathcal{F},\kappa)$ and mismatch cases $r^{p-1}(\mathcal{F},\kappa)=F^{p-1}\bar{x}^{p-1}(\mathcal{F},\kappa)$

can be obtained, and then the control inputs under match case $u^p(\mathcal{F},\kappa)=u^p(\mathcal{F},\kappa-1)+r^p(\mathcal{F},\kappa)$ and mismatch case $u^{p-1}(\mathcal{F},\kappa)=u^{p-1}(\mathcal{F},\kappa-1)+F^{p-1}(\bar{\boldsymbol{a}}^{p-1})^{-1}\bar{x}^p(\mathcal{F},\kappa)$ are obtained. Next, by utilizing the control input, system (2) is updated. Meanwhile, the Max-DT and Min-DT are obtained by (47) in real time.

Step 3: To determine if the system state switching condition $\gamma^{p+1}(x(\mathcal{F},\kappa))$ is satisfied, and if so, the system state will move to the next phase, otherwise return to step 2. Meanwhile, if $t\leq$(Min-DT)-(Max-DT) is met, the advanced signal is immediately given (i.e., ensuring the state and controller switching occurs simultaneously.), otherwise, return to step 2.

Step 4: The system into the next phase, repeat step 1.

IV. Simulation Study

A. Simulation Study

In this section, we take the case of the injection molding process mentioned in [24] as an example. In the injection molding process case study of this article, the switching control from the injection phase to the pressure holding phase is used to verify the effectiveness and feasibility of the developed method. According to [24], the injection phases' model is:

$$\begin{cases}\mathrm{IV}(\mathcal{F}+1,\kappa)=0.9291\mathrm{IV}(\mathcal{F},\kappa)+8.687\mathrm{VO}(\mathcal{F},\kappa)\\ \qquad\qquad +(0.03191\mathrm{IV}(\mathcal{F}-1,\kappa)-5.617\mathrm{VO}(\mathcal{F}-1,\kappa))\\ \mathrm{NP}(\mathcal{F}+1,\kappa)=\mathrm{NP}(\mathcal{F},\kappa)+0.1054\mathrm{IV}(\mathcal{F},\kappa)\\ \qquad\qquad (0.004\mathrm{IV}(\mathcal{F},\kappa)+1)\end{cases} \tag{58}$$

where $\mathrm{IV}(\mathcal{F},\kappa)$, $\mathrm{VO}(\mathcal{F},\kappa)$ and $\mathrm{NP}(\mathcal{F},\kappa)$ are the injection velocity, valve opening, and nozzle pressure, respectively.

And the pressure holding phase is:

$$\begin{aligned}\mathrm{NP}(\mathcal{F}+1,\kappa)&=1.317\mathrm{NP}(\mathcal{F},\kappa)+171.8VO(\mathcal{F},\kappa)\\ &\quad-(0.3259\mathrm{NP}(\mathcal{F}-1,\kappa)+156.8\mathrm{VO}(\mathcal{F}-1,\kappa))\end{aligned} \tag{59}$$

Define

$$\begin{aligned}x^1(\mathcal{F},\kappa)&=[\mathrm{IV}(\mathcal{F},\kappa)0.03191\mathrm{IV}(\mathcal{F}-1,\kappa)\\ &\quad-5.617\mathrm{VO}(\mathcal{F}-1,\kappa)\\ &\mathrm{NP}(\mathcal{F},\kappa)],u^1(\mathcal{F},\kappa)=\mathrm{VO}(\mathcal{F},\kappa),\ y^1(\mathcal{F},\kappa)=\mathrm{IV}(\mathcal{F},\kappa),\\ x^2(\mathcal{F},\kappa)&=[\mathrm{NP}(\mathcal{F},\kappa)(0.3259\mathrm{NP}(\mathcal{F}-1,\kappa)\\ &\quad+156.8\mathrm{VO}(\mathcal{F}-1,\kappa))],\\ u^2(\mathcal{F},\kappa)&=\mathrm{VO}(\mathcal{F},\kappa),\ y^2(\mathcal{F},\kappa)=\mathrm{NP}(\mathcal{F},\kappa).\end{aligned}$$

we have

$$\begin{aligned}x^1(\mathcal{F}+1,\kappa)&=\begin{bmatrix}x^{11}(\mathcal{F}+1,\kappa)\\ x^{12}(\mathcal{F}+1,\kappa)\\ x^{13}(\mathcal{F}+1,\kappa)\end{bmatrix}\\ &=\begin{bmatrix}y^1(\mathcal{F}+1,\kappa)\\ 0.3191y^1(\mathcal{F},\kappa)-5.617u^1(\mathcal{F},\kappa)\\ y^2(\mathcal{F}+1,\kappa)\end{bmatrix}\\ &=\begin{bmatrix}0.9291&1&0\\ 0.03191&0&0\\ 0.1054&0&1\end{bmatrix}\\ &\quad\times\begin{bmatrix}y^1(\mathcal{F},\kappa)\\ 0.3191y^1(\mathcal{F}-1,\kappa)-5.617u^1(\mathcal{F}-1,\kappa)\\ y^2(\mathcal{F},\kappa)\end{bmatrix}\\ &\quad+\begin{bmatrix}8.687\\ -5.617\\ 0\end{bmatrix}u^1(\mathcal{F},\kappa)\end{aligned} \tag{60}$$

$$\begin{aligned}x^2(\mathcal{F}+1,\kappa)&=\begin{bmatrix}x^{21}(\mathcal{F}+1,\kappa)\\ x^{22}(\mathcal{F}+1,\kappa)\end{bmatrix}\\ &=\begin{bmatrix}y^2(\mathcal{F}+1,\kappa)\\ 0.3259y^2(\mathcal{F},\kappa)-156.8u^2(\mathcal{F},\kappa)\end{bmatrix}\\ &=\begin{bmatrix}1.317&1\\ -0.3259&0\end{bmatrix}\\ &\quad\times\begin{bmatrix}y^2(\mathcal{F},\kappa)\\ 0.3259y^2(\mathcal{F}-1,\kappa)-156.8u^2(\mathcal{F}-1,\kappa)\end{bmatrix}\\ &\quad+\begin{bmatrix}171.8\\ -156.8\end{bmatrix}u^2(\mathcal{F},\kappa)\end{aligned} \tag{61}$$

Then, the state space model of injection phase is

$$\begin{cases}x^1(\mathcal{F}+1,\kappa)=A^1(\mathcal{F},\kappa)x^1(\mathcal{F},\kappa)\\ +B^1(\mathcal{F},\kappa)u^1(\mathcal{F},\kappa)+\omega(\mathcal{F},\kappa)\\ y^1(\mathcal{F},\kappa)=C^1x^1(\mathcal{F},\kappa)\end{cases} \tag{62}$$

where 1 denotes the system running in the injection phase.

Furthermore, under the time-delay situation, (55) can be transformed into the below form.

$$\begin{cases}x^1(\mathcal{F}+1,\kappa)=\sum_{\mathcal{G}=-2}^{0}A^1_{\mathcal{G}}(\mathcal{F},\kappa)x^1(\mathcal{F}+\mathcal{G},\kappa)\\ +B^1(\mathcal{F},\kappa)u^1(\mathcal{F},\kappa)+\omega^1(\mathcal{F},\kappa)\\ y^1(\mathcal{F},\kappa)=C^1x^1(\mathcal{F},\kappa)\end{cases} \tag{63}$$

where $A^1_g(\mathcal{F},\kappa)=A^1_g+N^1\Delta^1(\mathcal{F},\kappa)H^1_a$, $B^1(\mathcal{F},\kappa)=B^1+N^1\Delta^1(\mathcal{F},\kappa)H^1_b$,

$$A^1_0=\begin{bmatrix}0.9291&1&0\\ 0.03191&0&0\\ 0.1054&0&1\end{bmatrix},A^1_{-1}=\begin{bmatrix}0.1&0.1&0\\ 0.2&0.1&0\\ 0.2&0&0.1\end{bmatrix},$$

$$A^1_{-2}=\begin{bmatrix}0.1&0.1&0\\ 0.2&0.1&0\\ 0.2&0&0.1\end{bmatrix},$$

$$B^1=\begin{bmatrix}8.687\\ -5.617\\ 0\end{bmatrix},N^1=\begin{bmatrix}0.1&0&0\\ 0&0.1&0\\ 0&0&0\end{bmatrix},$$

$$H^1_a=\begin{bmatrix}0.104&0&0\\ 0.5&0&0\\ 0&0&0\end{bmatrix},\ H^1_b=0.005\times B^1,$$
$$C^1=\begin{bmatrix}1&0&0\end{bmatrix},$$

$\omega^1(\mathcal{F},\kappa)=[\Delta^1(\mathcal{F},\kappa)\Delta^2(\mathcal{F},\kappa)\Delta^3(\mathcal{F},\kappa)]^{\mathrm{T}}$, $\Delta^i(\mathcal{F},\kappa)\in[-1,1]$, $i=1,2,3,4,5$.

TABLE I
COMPUTATIONAL COMPLEXITY COMPARISON

	Reference [17] with LKF	Reference [27] with LKF	Developed method with LRF
The number of free weighting matrixes (Q)	11	11	1
The LMI conditions dimensionality (k)	13	15	8
Numerical complexity ($X=Qk^3$)	24167	37125	512
CPU calculation time for LMI conditions	1.03s	1.62s	0.015s

Similarly, the model for pressure holding phase is

$$\begin{cases} x^2(\mathcal{F}+1,\kappa) = A^2(\mathcal{F},\kappa)x^2(\mathcal{F},\kappa) \\ +B^2(\mathcal{F},\kappa)u^2(\mathcal{F},\kappa)+\omega(\mathcal{F},\kappa) \\ y^2(\mathcal{F},\kappa) = C^2x^2(\mathcal{F},\kappa) \end{cases} \tag{64}$$

where 2 denotes the system running in the pressure holding phase. Considering the time-delay, (65) can be obtained.

$$\begin{cases} x^2(\mathcal{F}+1,\kappa) = \sum_{\mathcal{G}=-2}^{0} A_{\mathcal{G}}^2(\mathcal{F},\kappa)x^2(\mathcal{F}+\mathcal{G},\kappa) \\ +B^2(\mathcal{F},\kappa)u^2(\mathcal{F},\kappa)+\omega^2(\mathcal{F},\kappa) \\ y^2(\mathcal{F},\kappa) = C^2x^2(\mathcal{F},\kappa) \end{cases} \tag{65}$$

where $A_{\mathcal{G}}^2(\mathcal{F},\kappa) = A_{\mathcal{G}}^2 + N^2\Delta^2(\mathcal{F},\kappa)H_a^2$, $B^2(\mathcal{F},\kappa) = B^2 + N^2\Delta^2(\mathcal{F},\kappa)H_b^2$ $A_0^2 = \begin{bmatrix} 1.317 & 1 \\ -0.3259 & 0 \end{bmatrix}$, $A_{-1}^2 = \begin{bmatrix} 0.1 & 0.1 \\ 0.2 & 0 \end{bmatrix}$, $A_{-2}^2 = \begin{bmatrix} 0.1 & 0.1 \\ 0.2 & 0 \end{bmatrix}$ $B^2 = \begin{bmatrix} 171.8 \\ -156.8 \end{bmatrix}$, $N^2 = \begin{bmatrix} 1 & 0 \\ 0 & 1 \end{bmatrix}$, $H_a^2 = \begin{bmatrix} 0.0104 & 0 \\ -0.0304 & 0 \end{bmatrix}$, $H_b^2 = 0.005 \times B^2$, $\omega^2(t,k) = C^1 = [1 \quad 0]$, $[\Delta^4(\mathcal{F},\kappa)\Delta^5(\mathcal{F},\kappa)]^{\mathrm{T}}$. In addition, when the switching occurs, the state of two adjacent phases satisfied.

$$\partial^1(x(\mathcal{F},\kappa)) = 350 - \begin{bmatrix} 0 & 0 & 1 \end{bmatrix} x^1(\mathcal{F},\kappa) < 0 \tag{66}$$

Then, the set values are $y_r^1 = 40$ (mm/s) in the 1st phase and $y_r^2 = 300$ (bar) in the 2nd phase.

Finally, a dynamic tracking indicator (DTI) is defined to describe the tracking performance. And the integral of absolute error (IAE) is defined to describe the overall tracking performance.

$$\mathrm{DTI} = \begin{cases} \sqrt{(e^{T_1})^{\mathrm{T}}e^{T_1}} 0 \le t < T_1 \\ \sqrt{(e^{T_2})^{\mathrm{T}}e^{T_2}} T_1 \le t \le T_1 + T_2 \end{cases} \tag{67}$$

$$\mathrm{IAE} = \int_0^{T_k} |e(\mathcal{F},\kappa)| d(\mathcal{F},\kappa) \tag{68}$$

B. Simulation Results

To demonstrate the lower computational effort of the developed method compared to the LKF methods [17], [27], the following comparison of the computational complexity is provided.

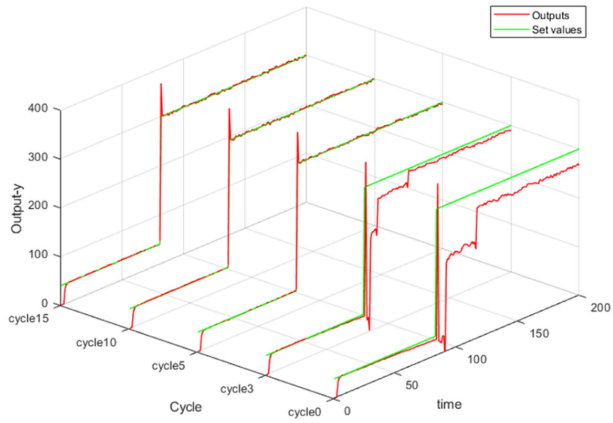

Fig. 2. Outputs of [24].

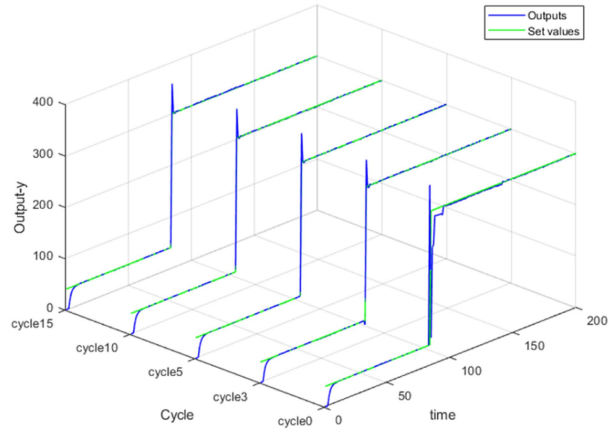

Fig. 3. Outputs of the developed method.

In Table I, we can see that the developed method has a lower computational complexity and shorter computational time than other LKF-based methods.

Remark 4: Currently, this work is only suitable for small time delay systems. Since the LRF method is based on a dimensional expansion approach, as the time delay increases, the dimensionality of the LMI conditions will subsequently become larger, which makes solving the LMI conditions extremely difficult, or even unsolvable.

Then, the uncertainties and unknow disturbances are considered in the simulation case. It is acceptable to compare the output, tracking error, and control input between the developed 2D-ILHRPC approach and the conventional 2D-ILC method [24] in the simulation study.

We repeatedly experimented with the trial-and-error method and finally chose the state weighting matrixes and tracking weighting matrix are selected as $Q_1^1 = \mathrm{diag}\ [10 \quad 8 \quad 4 \quad 1]$, $Q_1^2 = \mathrm{diag}[10 \quad 2.5 \quad 9]$, $R_1 = 0.1$, and $R_2 = 0.1$. In addition, in the simulation results, we use an operation cycle to represent a batch.

Figs. 2 and 3 show the tracking effect of the output for the developed method and [24], respectively. The set values of the injection and pressure holding phases are 40 mm/s and 300

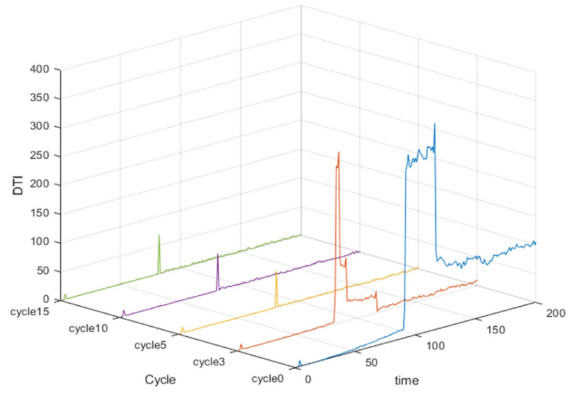

Fig. 4. DTI curves of the [24].

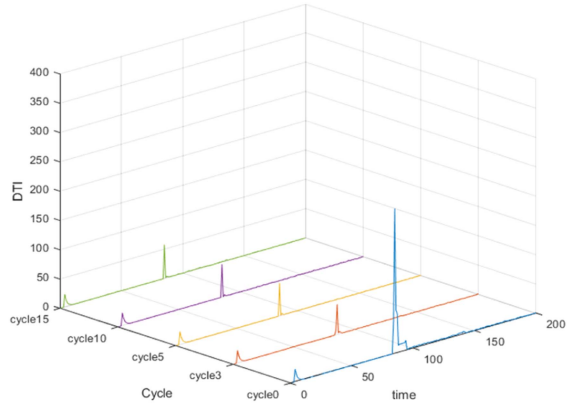

Fig. 5. DTI curves of the developed method.

bar, respectively. Fig. 2 clearly shows the tracking effect of [24] for the previous 20 batches, in which the 3rd batch and the 5th batch have large tracking errors, and the system is not able to track the set values consistently until the 10th batch. The developed method, which considers both time information and batch information, is able to track the set values stably in the fifth batch. In contrast, the developed method has fewer learning cycles. This means that the equipment is able to produce more high-quality products in less time. In addition, the system switches from the injection to the pressure holding phases when pressure value reaches 350 (bar) according to (66). However, the holding phases' set value is 300 (bar), so a spike occurs during switching.

Figs. 4 and 5 show the DTI of the developed method and [24], respectively. Obviously, the developed method has much better tracking performance before the 5th batch. Meanwhile, the DTI of two methods at the switching point is exhibited. In comparison, the DTI of the developed method is about 14.9% lower than [24] at the switching point, which is smoother and more stable during the switching process.

In addition, according to Table II, before the 5th batch, the average DTI of the developed method is significantly lower than [24]. After the 10th batch, i.e., entering the steady state, the average DTI of the developed method is about 30% lower than

TABLE II
AVERAGE DTI OF TWO METHODS

	Developed method	Reference [24]
3rd batch	4.2206	82.1700
5th batch	1.0402	16.5447
10th batch	0.9225	1.3686
15th batch	0.9384	1.3642
20th batch	0.9255	1.3543

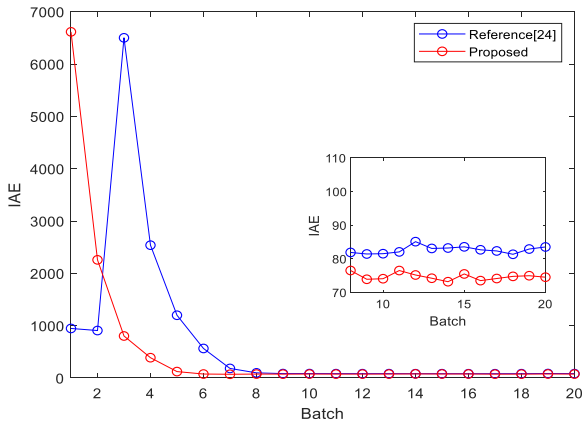

Fig. 6. IAE of the developed method and [24].

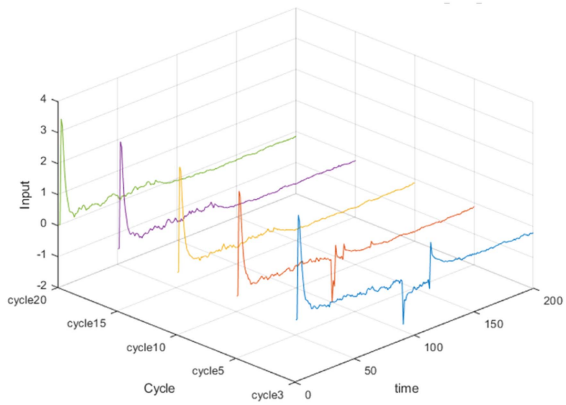

Fig. 7. Control inputs of the [24].

[24]. The lower the DTI means the higher productivity and lower scrap rates.

Fig. 6 is the IAE of the developed method and [24]. The developed method achieves a steady state in shorter batches. Especially, after the 8th batch (two methods can operate stably), the IAE of the developed method is still smaller than [24]. This indicates the developed method has a better overall tracking performance.

Figs. 7 and 8 display the control input of the developed method and [24], respectively. By comparison, it is easy to see that the control input's fluctuation with the developed method is smaller than [24] in both the injection and holding phases. When switching occurs, due to the change in control objectives, the control input has fluctuated, but the developed method has still a smaller fluctuation than [24]. That's friendly to the actuator, because a smaller fluctuation of the control input means less

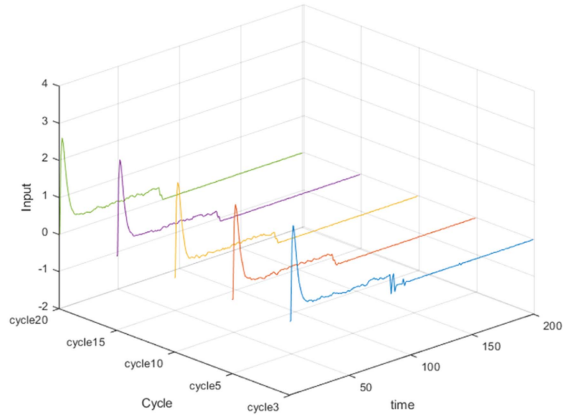

Fig. 8. Control inputs of the developed method.

actuator action. The life of the actuator can be made to last longer, and the cost of the equipment can be cut.

Remark 5: In the injection molding process, the injection and the pressure holding phases are the two most critical parts. In the injection phase, the injection speed is the key factor that affects the production efficiency. In the pressure-holding phase, the stable pressure ensures the product's quality. If the injection speed does not reach the set values, the production efficiency will be seriously reduced. If the cavity pressure is not sufficient, the product quality will also be severely compromised and become scrap.

V. Conclusion

A 2D ILHRPC approach is developed for MPBP with small time-delays and asynchronous switching. First, by using the state deviation and output error, a novel 2D Roesser comprehensive feedback error switching model is constructed, which is utilized to design an ILHRPC law. Second, combining the stability conditions, which are given by the terminal constraints set, and the exponential stability analysis, the real-time gains of the control law, Min-DT, and the Max-DT, are solved. Based on the dwelling times, the advanced signal is given to ensure the system's stability when switching occurs. The simulation results finally display that the developed approach is effective and feasible. Due to the increasing complexity of modern production processes, the operational burden on actuators is also increasing, which leads to inevitable actuator fault problems. In the future, we will further investigate MPBP with actuator fault.

References

[1] T. Pinto. Varela, A. Barbosa. Povoa, and A. Carvalho, "Sustainable batch process retrofit design under uncertainty an integrated methodology," *Comput. Chem. Eng.*, vol. 102, pp. 226–237, Jul. 2017.

[2] C. Han, L. Jia, and D. Peng, "Model predictive control of batch processes based on two-dimensional integration frame," *Nonlinear Anal.: Hybrid Syst.*, vol. 28, pp. 75–86, Nov. 2018.

[3] X. Liu, L. Ma, X. Kong, and K. Y. Lee, "An efficient iterative learning predictive functional control for nonlinear batch processes," *IEEE Trans. Cybern.*, vol. 52, no. 6, pp. 4147–4160, Oct. 2020.

[4] X. Wen, H. Y. Shi, C. L. Su, X. Y. Jiang, P. Li, and J. X. Yu, "Novel data-driven two-dimensional Q-learning for optimal tracking control of batch process with unknown dynamics," *ISA Trans.*, vol. 125, pp. 10–21, Jun. 2022.

[5] F. Chu, J. Wang, Y. Wang, G. Chai, R. Jia, and F. Wang, "Integrated operation optimization strategy for batch process based on process transfer model under disturbance," *Can. J. Chem. Eng.*, vol. 101, no. 1, pp. 368–379, 2023.

[6] L. Ma, X. Liu, F. Gao, and K. Y. Lee, "Event-based switching iterative learning model predictive control for batch processes with randomly varying trial lengths," *IEEE Trans. Cybern.*, early access, Jan. 26, 2023, doi: 10.1109/TCYB.2023.3234630.

[7] J. Shi, F. R. Gao, and T. J. Wu, "Robust iterative learning control design for batch processes with uncertain perturbations and initialization," *AICHE J.*, vol. 52, no. 6, pp. 2171–2187, Apr. 2006.

[8] Y. Q. Wang, H. Zhang, S. L. Wei, D. H. Zhou, and B. Huang, "Control performance assessment for ILC-controlled batch processes in a 2-D system framework," *IEEE Trans. Syst. Man Cybern.-Syst.*, vol. 48, no. 9, pp. 1493–1504, Sep. 2018.

[9] D. Meng and J. Zhang, "Robust optimization-based iterative learning control for nonlinear systems with nonrepetitive uncertainties," *IEEE/CAA J. Automatica Sinica*, vol. 8, no. 5, pp. 1001–1014, May 2021.

[10] Z. K. Nagy and R. D. Braatz, "Robust nonlinear model predictive control of batch processes," *AIChE J.*, vol. 49, no. 7, pp. 1776–1786, Apr. 2003.

[11] R. Zhang, S. Wu, Z. Cao, J. Lu, and F. Gao, "A systematic min-max optimization design of constrained model predictive tracking control for industrial processes against uncertainty," *IEEE Trans. Control Syst. Technol.*, vol. 26, no. 6, pp. 2157–2164, Nov. 2018.

[12] R. Zhang, R. Lu, A. Xue, and F. Gao, "New minmax linear quadratic fault-tolerant tracking control for batch processes," *IEEE Trans. Autom. Control*, vol. 61, no. 10, pp. 3045–3051, Oct. 2016.

[13] S.-K. Oh and J. M. Lee, "Iterative learning model predictive control for constrained multivariable control of batch processes," *Comput. Chem. Eng.*, vol. 93, pp. 284–292, Oct. 2016.

[14] L. Jia, C. Han, and M. S. Chiu, "Dynamic R-parameter based integrated model predictive iterative learning control for batch processes," *J. Process Control*, vol. 49, pp. 26–35, Jan. 2017.

[15] R. D. Zhang and F. R. Gao, "Two-dimensional iterative learning model predictive control for batch processes: A new state space model compensation approach," *IEEE Trans. Syst., Man, Cybern.: Syst.*, vol. 51, no. 2, pp. 833–841, Feb. 2021.

[16] Y. Q. Wang, D. H. Zhou, and F. R. Gao, "Iterative learning model predictive control for multi-phase batch processes," *J. Process Control*, vol. 18, no. 6, pp. 543–557, Jul. 2008.

[17] L. M. Wang, Y. T. Shen, J. X. Yu, P. Li, R. D. Zhang, and F. R. Gao, "Robust iterative learning control for multi-phase batch processes: An average dwell-time method with 2D convergence indexes," *Int. J. Syst. Sci.*, vol. 49, no. 2, pp. 324–343, Nov. 2018.

[18] S. Zhang, C. Zhao, and F. Gao, "Incipient fault detection for multiphase batch processes with limited batches," *IEEE Trans. Control Syst. Technol.*, vol. 27, no. 1, pp. 103–117, Jan. 2017.

[19] B. Peng, H. Y. Shi, C. L. Su, and P. Li, "Robust switched predictive control for multi-phase batch processes with uncertainties and unknown disturbances," *J. Process Control*, vol. 94, pp. 110–124, Oct. 2020.

[20] H. Zhang, X. Tian, X. Deng, and Y. Cao, "Multiphase batch process with transitions monitoring based on global preserving statistics slow feature analysis," *Neurocomputing*, vol. 293, pp. 64–86, Jun. 2018.

[21] B. Peng, H. Y. Shi, C. L. Su, X. Wen, and P. Li, "Robust asynchronous switching predictive control for multi-phase batch processes with time-varying tracking trajectory and delay," *Int. J. Control*, vol. 96, pp. 645–668, Nov. 2023.

[22] H. Li, L. J. Song, X. Y. Jiang, H. Y. Shi, C. L. Su, and P. Li, "Robust model predictive control for multi-phase batch processes with asynchronous switching," *Int. J. Control, Automat. Syst.*, vol. 20, no. 1, pp. 84–98, Mar. 2022.

[23] C. Zhou, L. Jia, and Y. Zhou, "A two-stage robust iterative learning model predictive control for batch processes," *ISA Trans.*, vol. 135, pp. 309–324, 2023.

[24] L. Wang, J. Yu, R. Zhang, P. Li, and F. Gao, "Iterative learning control for multiphase batch processes with asynchronous switching," *IEEE Trans. Syst. Man Cybern.-Syst.*, vol. 51, no. 4, pp. 2536–2549, Apr. 2021.

[25] C. Hua, T. Zhang, Y. Li, and X. Guan, "Robust output feedback control for fractional order nonlinear systems with time-varying delays," *IEEE/CAA J. Automatica Sinica*, vol. 3, no. 4, pp. 477–482, Oct. 2016.

[26] W. Yu, J. Song, and J. Yu, "Robust hybrid controller design for batch processes with time delay and its application in industrial processes," *Int. J. Control, Automat. Syst.*, vol. 17, no. 11, pp. 2881–2894, Nov. 2019.
[27] H. Y. Shi, P. Li, J. T. Cao, C. L. Su, and J. X. Yu, "Robust fuzzy predictive control for discrete-time systems with interval time-varying delays and unknown disturbances," *IEEE Trans. Fuzzy Syst.*, vol. 28, no. 7, pp. 1504–1516, Jul. 2020.
[28] L. Wang, J. Song, R. Zhang, and F. Gao, "Constrained model predictive fault-tolerant control for multi-time-delayed batch processes with disturbances: A Lyapunov-Razumikhin function method," *J. Franklin Inst.*, vol. 358, no. 18, pp. 9483–9509, Dec. 2021.
[29] L. Teng, Y. Wang, W. Cai, and H. Li, "Robust model predictive control of discrete nonlinear systems with time delays and disturbances via T–S fuzzy approach," *J. Process Control*, vol. 53, pp. 70–79, May 2017.
[30] L. Teng, Y. Wang, W. Cai, and H. Li, "Efficient robust fuzzy model predictive control of discrete nonlinear time-delay systems via Razumikhin approach," *IEEE Trans. Fuzzy Syst.*, vol. 27, no. 2, pp. 262–272, Feb. 2019.
[31] K. Yu and C. Lien, "Stability criteria for uncertain neutral systems with interval time-varying delays," *Chaos Solitons Fractals*, vol. 38, no. 3, pp. 650–657, Nov. 2008.
[32] J. Geromel, P. D. Peres, and J. Bernussou, "On a convex parameter space method for linear control design of uncertain systems," *SIAM J. Control Optim.*, vol. 29, no. 2, pp. 381–402, 1991.
[33] S. Boyd, L. El Ghaoui, E. Feron, and V. Balakrishnan, *Linear Matrix Inequalities in System and Control Theory*. Philadelphia, PA, USA: SIAM, 1994.

Hui Li received the M.S. degree in control theory and control engineering from Liaoning Petrochemical University, Fushun, China, in 2021. He is currently working toward the Ph.D. degree in control theory and control engineering from the University of Science and Technology Liaoning, Anshan, China. His research interests include multi-phase switching control, iterative learning control, robust model predictive control, and fault-tolerant control.

Shiqi Wang received the M.S. degree in control theory and control engineering from Liaoning Petrochemical University, Fushun, China, in 2021. She is currently working toward the Ph.D. degree in control theory and control engineering from the University of Science and Technology Liaoning, Anshan, China. Her research interests include advanced process control, output feedback control, and robust model predictive control.

Huiyuan Shi received the Ph.D. degree in control theory and control engineering from Northwestern Polytechnical University, Xi'an, China, in 2020. He is currently holding a Postdoctoral position with the State Key Laboratory of Integrated Automation for Process Industries, Northeastern University, Boston, MA, USA. He is also an Associate Professor with the School of Information and Control Engineering, Liaoning Petrochemical University, Fushun, China. His research interests include robust predictive control, advanced process control, and data-based control.

Ping Li (Senior Member, IEEE) received the Ph.D. degree in automatic control from Zhejiang University, Hangzhou, China, in 1995. He is currently a Full Professor of the University of Science and Technology Liaoning, Anshan, China. He has successfully completed more than 20 research projects supported by national and ministry funds. His research interests include process control and automation and predictive control. He was the recipient of more than ten awards of the nation and ministry.

Chengli Su (Member, IEEE) received the Ph.D. degree in control science and engineering with the College of Information Science & Engineering, Zhejiang University, Hangzhou, China, in 2006. Since 2006, he has been with the School of Information and Control Engineering, Liaoning Petrochemical University, China, as a Professor. He is also with the School of Information Engineering, Liaodong University, Dandong, China. His research interests include advanced control and optimization of complex petrochemical process, predictive control, and fuzzy control.